UNIVERSIDAD DE INVESTIGACIÓN DE TECNOLOGÍA EXPERIMENTAL YACHAY

Escuela de Ciencias Biológicas e Ingeniería

TÍTULO: Design of Prototype of Myoelectric Hand Prosthesis

Trabajo de integración curricular presentado como requisito
para la obtención del título de Ingeniera Biomédica

Autor:

Ortiz Vinueza Lizbeth Dayanara

Tutor:

Mgs. Villalba Meneses Gandhi Fernando

Urcuquí, Julio 2023

AUTORÍA

Yo, **LIZBETH DAYANARA ORTIZ VINUEZA**, con cédula de identidad 1720131166, declaro que las ideas, juicios, valoraciones, interpretaciones, consultas bibliográficas, definiciones y conceptualizaciones expuestas en el presente trabajo; así como, los procedimientos y herramientas utilizadas en la investigación, son de absoluta responsabilidad de él/la autor(a) del trabajo de integración curricular. Así mismo, me acojo a los reglamentos internos de la Universidad de Investigación de Tecnología Experimental Yachay.

Urcuquí, 21 de Julio de 2023.

_____

Lizbeth Dayanara Ortiz Vinueza
CI: 1720131166

AUTORIZACIÓN DE PUBLICACIÓN

Yo, **LIZBETH DAYANARA ORTIZ VINUEZA**, con cédula de identidad 1720131166, cedo a la Universidad de Investigación de Tecnología Experimental Yachay, los derechos de publicación del presente trabajo de integración curricular, sin que deba haber un reconocimiento económico por este concepto. Declaro además que el texto del presente trabajo de titulación no podrá ser cedido a ninguna empresa editorial para su publicación u otros fines, sin contar previamente con la autorización escrita de la Universidad.

Asimismo, autorizo a la Universidad que realice la digitalización y publicación de este trabajo de integración curricular en el repositorio virtual, de conformidad a lo dispuesto en el Art. 144 de la Ley Orgánica de Educación Superior.

Urcuquí, 21 de Julio de 2023.

_____

Lizbeth Dayanara Ortiz Vinueza

CI:17201131166

DEDICATION

To my parents, Cesar and Sandra,
who has helped me to overcome many obstacles.
For teaching me that those who persevere
achieve their goals and dreams.
For always demonstrating me that effort will rewarded
no matter how difficult the road is.

ACKNOWLEDGEMENTS

I want to thank you for the motivation, guidance, and support during the development of this project that I received from my thesis advisor, Fernando Ghandi Villalba Meneses, Ph.D.

I want to thank God for the gift of life and for allowing me to finish bachelor degree studies. Also, I am incredibly grateful to my parents, who support me with unconditional love, and their lifelong guidance and help me in difficult moments. I want to thank a special person who stole my heart, Santiago, who always encouraged me to move forward.

Likewise, Thank you to the School of Biological Sciences and Engineering professors for their commitment, patience, and support. I built a world full of knowledge and love for science with you. Also, to Yachay Tech University, where I received the best training and prepared myself professionally and for life.

Finally, I thank my friends who became my second family and believed in my abilities Gabriela, Xiomara, José, Mirian, Stefany and Daniela. With them I learned that we all have different processes.

With gratitude,

Lizbeth Ortiz Vinueza

RESUMEN

Después de perder una extremidad superior, los pacientes sufren una discapacidad permanente que puede requerir la asistencia de otros. En la actualidad, se han propuesto varios dispositivos protésicos para recuperar la parte física y motora de pacientes con discapacidad, amputaciones o enfermedades congénitas. Sin embargo, los altos costos de las prótesis mioeléctricas comerciales están bloqueando la accesibilidad, sobre todo para los países subdesarollados como el Ecuador. Este trabajo de investigación propone y desarrolla un diseño 3D funcional y de bajo costo de una prótesis de mano mioeléctrica que combina métodos computacionales y principios electrónicos para que las mujeres se adapten a tareas relacionadas con actividades de la vida diaria (AVD) proporcionándoles una mejor calidad de vida. Este estudio tiene gran relevancia debido al limitado acceso a nivel nacional de una tecnología capaz de controlarse a través de las señales de activación muscular como un método más natural y eficiente en el tiempo. Gracias a los avances relacionados a la tecnología de impresión 3D, se emplea el filamento termoplástico ABS para la fabricación de la palma rígida, los cinco dedos, el socket del antebrazo y, el circuito electrónico. El modelo ensamblado presenta un peso aproximado de 404 gramos, tiene dos grados de libertad (GDL) y es semejante a la biomecánica de la mano humana con un total de catorce articulaciones. Este diseño permite simular el movimiento de agarre de precisión abierto, cilíndrico y de punta. Por otra parte, se selecciona el Arduino UNO como sistema de control, se implementan micro servomotores para mover los dedos como parte de la actuación y se selecciona una Li-Po batería recargable para suministrar energía. El prototipo es controlado a través de señales electromiográficas (EMG) que se procesan con la interfaz del software LabVIEW. Además, con el fin de garantizar un prototipo útil y estable junto con la identificación de posibles deficiencias del modelo, se realiza el análisis de elementos finitos utilizando el software SimSolid. Con los resultados obtenidos se estudia la distribucion de las tensiones en el área de las falanges y los bordes distales del prototipo, evidenciando los mayores puntos de contacto y la magnitud de la fuerza.

Palabras clave: Prótesis mioeléctrica de mano, Análisis estructural, Movimientos de Agarre, Señales EMG, SimSolid, LabVIEW, Análisis de Elementos Finitos.

ABSTRACT

After losing an upper limb, patients suffer a permanent disability that may require others' assistance. Nowadays, several prosthetic devices have been proposed to recover the physical and motor part of patients with disabilities, amputations, or congenital diseases. However, the high costs of commercial myoelectric prostheses are blocking accessibility, especially for underdeveloped countries like Ecuador. This research project proposed and developed a functional and low-cost 3D design of a myoelectric hand prosthesis that combines computational methods and electronic principles for women to adapt to tasks related to activities of daily living (ADL), providing them with a better quality of life. This study is highly relevant due to the limited national access to a technology capable of being controlled through muscle activation signals as a more natural and time-efficient method. Thanks to advances in 3D printing technology, ABS thermoplastic filament is used to manufacture the rigid palm, the five fingers, the forearm socket, and the electronic circuit. The assembly model weighs approximately 404 grams, has two degrees of freedom (DoF), and resembles the human hand biomechanism with fourteen joints. This design simulates the motion of precision open, cylindrical, and tip grasping tasks. Moreover, Arduino UNO is selected as the control system, micro servo motors are implemented to operate the fingers as the actuation setup and a rechargeable Li-Po battery is selected to supply power. The prototype is controlled through electromyography (EMG) signals processed with the LabVIEW software interface. In order to ensure a valuable and stable prototype, together with the identification of possible shortcomings of the model, a finite element analysis is performed using SimSolid software. The results allow analysis of stress distributions in the distal and proximal phalanx, and the distal edges of the prototype are studied, evidencing the more significant points of contact and the magnitude of force.

Keywords: Myoelectric hand prosthesis, Structural Analysis, Tasking grasp, EMG signals, SimSolid, LabVIEW, Finite Elements Analysis.

Contents

X

List of Figures

List of Tables

List of Abbreviations

3D Three Dimensions or Three Dimensional. 2, 4, 31, 34, 39, 53, XI

ABS Acrylonitrile Butadiene Styrene. 3, 28, 30, 34, 41, 43, 46, 48, 53, 54
ADC Analogue to Digital Converter. 17, 38
ADL Activities of Daily Life. 1, 3, 59
ANN Artificial Neutral Networks. 57
AR Augmented Reality. 20

CAD Computer-Aided Design. 4, 31, 33, 41, 47, 53, 56, XI, XII
CE Concurrent Engineering. 25, 28, 59
CMC Carpometacarpal Joint. 7
CNS Central Nervous System. 16, 55
CONADIS Consejo Nacional de Discapacidades. 2

DC Direct Current. 54
DIP Distal Interphalangeal Joint. 7, 9, 26, 32, 42
DoF Degrees of Freedom. 1, 6, 7, 18, 42, 59, 60

ECG Electrocardiogram. 56
EDC Extensor Digitorum Communis. 17, 38
EMG Electromyography. 15–17, 19, 20, 25, 37–39, 41, 51–53, 55, 57, 58, XII

FDS Flexor Digitorum Superficialis. 17, 38
FEM Finite Elements Method. 3

GDP Gross Domestic Product. 19

IMC Intermetacarpal Joint. 9

LDA Linear Discriminant Analysis. 57
LiPo Lithium-ion Polymer. 37, 56, 59

MCP Metacarpophalangeal Joint. 7, 9, 26, 31, 32, 42
MCU's Microcontrollers. 18, 55, 56
MES Myoelectric Signals. 15, 16
MUP Motor Unit Potential. 16

NiMH Nickel Metal Hydride battery. 56

PCB Printed circuit board. 18, 19

Chapter 1

Introduction

The primary organ for manipulating objects through pressure and touch is thought to be the human hand. Anatomically, the hand is very complex and has many degrees of freedom (DoF) due to the various tasks it performs daily, such as grasping and object manipulations[1]. In addition, the variety of sensory receptors and the complex communication with the brain have allowed it to be the main challenge for the patient's physical rehabilitation[2].

The German book Ersatzglieder und Arbeitshilfen (Substitute Limbs and Work Aids), written by G. Schlesinger and published in 1919, was the first work to discuss the idea of powering a prosthesis externally[3]. Years later, there have been impressive advances in upper limb prosthetics, which competed according to their functionality and speed, such as the prototype of prosthetic hand created by Jacob Hüfner in Germany in 1922[4]. With advances in technology, the concept of myoelectric prosthesis was introduced and Reinhold Reiter created the first myoelectric prosthesis in 1948[5]. As expected, the first myoelectric prostheses that were developed were not functional or practical, had large sizes, heavy weights, too slow speed and the pinching force was very limited[6].

Over the years myoelectric prostheses have progressively improved in functionality. The myoelectric prosthesis was a viable clinical option for rehabilitation by 1980[6]. According to the studies of Biddiss and Chau carried out in 2007, during those previous 25 years the prostheses with a myoelectric mode of action became one of the most functional options and with the best cosmetic appearance, however about 23% of the rates referred to the abandonment of prostheses[7]. Through the years, multiple improvements to myoelectric prostheses are found. Undoubtedly, the increase in joints and actuators is one of the most successful improvements[8]. Each time different grips are added to give the prosthetic hands greater functionality, dexterity in activities of daily life (ADL) as well as impressive improvements at the aesthetic and cosmetic level that make the appearance more realistic[9]. However, one of the features that has not been completely improved over the years is costs, so acquiring a prosthesis for many is not an option.

1.1   Problem Statement

After losing an upper limb, patients suffer a permanent disability that may require others' assistance. Nowadays, several prosthetic devices have been proposed to recover patient's independence. There are designs more sophisticated, ergonomic, and aesthetic to help millions of amputees every year. Finding customized prosthetic solutions for people with disability, amputations, or congenital diseases of the upper

limb has become necessary to meet their requirements without affecting their functionality and foremost to improve the patient's quality of life. For this reason, prostheses are designed to restore functionality to the upper extremity providing a range of motion with a cosmetic appearance[10]. Actually, there are several commercially available prostheses such as Vincent Hand developed by Vincent Systems, Michelangelo and Bebionic Hand created by Otto Bock, and i-Limb® Hand by Touch Bionics. Despite the multiple benefits, these designs also present several problems associated with kinematic functionalities[10], adaptability and durability.[11].

Furthermore, according to the research of Calado et al. (2019) where commercial myoelectric upper limb prostheses were reviewed, the lowest cost was 6600 USD[12]. As a consequence, the high costs of commercial myoelectric prostheses are blocking the accessibility, above all for developing countries[13]. Unfortunately, traumatic amputation occurs more frequently in developing countries than in developed nations and only a reduced part of the population is partially covered with health insurance[14]. Consequently, the commercial myoelectric prosthesis that is now on the market only benefits a small proportion of the world's amputee population in countries with more financial resources.

All of the above is reflected in the document issued by the World Health Organization (WHO) where around 40 million people worldwide need a prosthesis, but only 5% or 15% have access to them[15] because most devices presented in the market turn out to be expensive and have limited access. In Ecuador, although there is no precise data on the level of amputations of the upper limb or hand, according to the Consejo Nacional de Discapacidades (CONADIS)[16], there is a registry of 471,205 people with a total rate of physical disability which means an approximately of 45.7% as shown in Figure 1.1.

Type of Disability
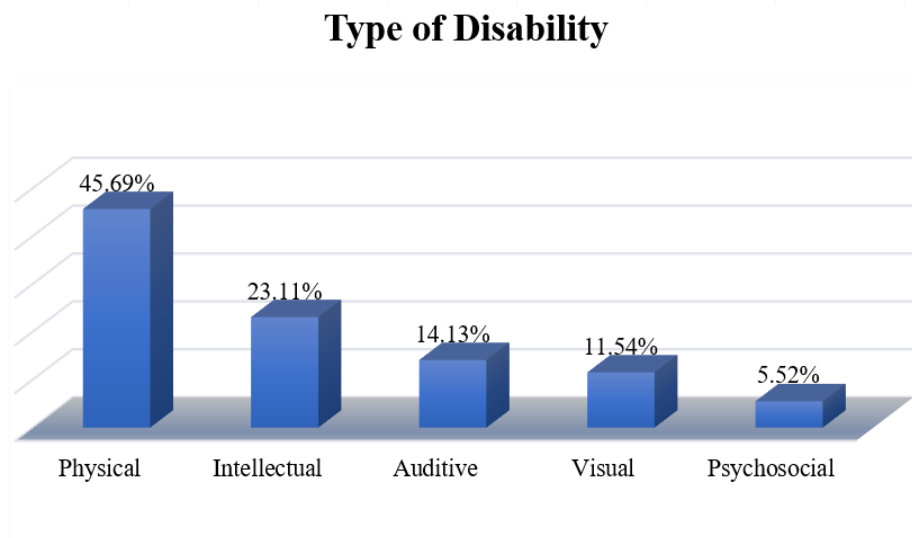
Figure 1.1: Statistics of the total number of people with disabilities in Ecuador. Adapted from CONADIS, 2021[16].

As a result, several public and private companies together with researchers have focused during the last decades to reduce the price of myoelectric prostheses. This has been achieved thanks to advances in 3D printing technology[17] and low costs of electronic components[18]. Due to the low cost, myoelectric prostheses are now in development trend, as has been seen. In Ecuador the vast majority of prostheses are

imported, but many of these do not fit the needs and the reality of each patient.

This study proposed and developed a functional and low-cost 3D design of a myoelectric hand prosthesis for women, which works similarly to the human hand. It aims to adapt to tasks related to activities of daily living (ADL) as well as the ergonomic and aesthetic demands of each user. It will allow returning the physical and motor part that has been lost, managing to simulate natural movements for the grasping of objects. Specifically, the developed design simulates the motion of a precision open grip, a cylindrical grip, and a tip grip. All components are connected internally with an electronic circuit that works safely for the user. Moreover, ABS plastic (Acrylonitrile Butadiene Styrene) was the material selected for 3D printing technology because it allows high mechanical resistance, durability, and flexibility. Also, it provides an aesthetic image because a filament color similar to the skin can be selected for the prototype of myoelectric hand prosthesis.

Finally, among the known shortcomings of other models are the lack of test and evaluation data in prosthesis development studies on the actual functionality of the prosthesis for ADL tasks. This study will provide a simulation stage that will allow to evaluate and test the prototype ensuring the development of a prosthesis that is functional and reliable for use in activities of daily life. The structural analysis of the prosthesis is performed through the finite elements method (FEM) with the use of Simsolid software which allows a general result of the behavior of the myoelectric hand prosthesis with different applied weights.

1.2 Justification

Among the most important needs that are sought to be solved with the modeling, construction and operation of upper limb prostheses, without affecting their functionality, are the acquisition costs and the similarity with the normal functions of a human hand. Currently, globally with the aim of recovering patient independence, there are several advanced designs with outstanding features that have helped thousands of patients. However, due to several factors mainly the economic in Ecuador the most commonly used prostheses for upper limbs are still purely mechanical or aesthetic. In this regard, the motivation arises to develop the present research work whose purpose is the development of a low-cost myoelectric prosthesis that allows adaptation to the activities of daily living as well as the ergonomic and aesthetic demands of each person. Thus, providing people with disabilities a better quality of life efficiently.

Therefore, the construction of the prototype of a myoelectric hand prosthesis is justified as a technology that is currently little or not developed in this country. In addition, to provide the patient with an affordable alternative to high-cost commercial options. The relevance of this research lies in the development from a new construction perspective, with a balance between technology, low cost and functionality thanks to the merging of engineering principles with the analysis of finite methods and advances in the manufacture of electronic components to meet specific user needs.

1.3   Research Objectives

1.3.1   General Objective

To design a functional and low-cost 3D prototype of myoelectric hand prosthesis, through the combination of computational methods and electronic principles that works similarly to the human hand to return the physical and motor part that has been lost.

1.3.2   Specific Objectives

- To use computer-aided design (CAD) software to create a design that allows the myoelectric hand prosthesis to manipulate objects and to ensure a useful and stable prototype.

- To evaluate the effects of forces and stress distribution through structural analysis in order to predict how the prototype will react and to be able to solve possible shortcomings.

- To provide a myoelectric interface that allows to the system detection to assure the total control of the prosthesis through the muscle activation signals in a more natural and time-efficient method.

- To design and evaluate a prototype of myoelectric hand prosthesis able to reproduce grips associated with stability and security such as precision open grip, cylindric grip, and tip grip.

1.4   Thesis Overview

This Project was organized as follows: Chapter 1 includes the problem statement, justification, general and specific objectives, and general thesis description. Followed by Chapter 2 contains the essential concepts related to the anatomy and motions of the human hand. The different methodologies for the biomechanical analysis of the hand were explained. In addition, it describes the acquisition of physiological signals EMG and the requirements for designing the prosthesis of a myoelectric hand. Also, the features of upper limb prostheses available in the market were mentioned. Chapter 3 contains the process carried out in this study and explains the different parameters and requirements for the prosthesis design. Chapter 4 contains the results of the main characteristics of the myoelectric hand prosthesis prototype, starting with the design requirements. This chapter ends with an interpretation of essential variables to system performance. Chapter 5 explains the discussion of the present research compared with similar works. Finally, chapters 6 and 7 contain the conclusions reached and future perspectives for the work to continue.

Chapter 2

State of the Art

2.1 Anatomy of the human hand

The hand is part of the human body's upper extremity, the central organ found in the distal extremity of the forearm[19], as shown in Figure 2.1 (obtained from Drake et.al[19]). The hand's ability to articulate with the rest of the body enables communication with the brain, which then integrates all the information and delivers a response to carry out tasks and allow interaction with the outside world. In addition, the hand is considered a mechanical, sensitive, and communicative tool that, thanks to its pressure and touch function, allows manipulation of objects and complex movements through the action of muscles inserted into the bones and of the ligaments that hold them[20].
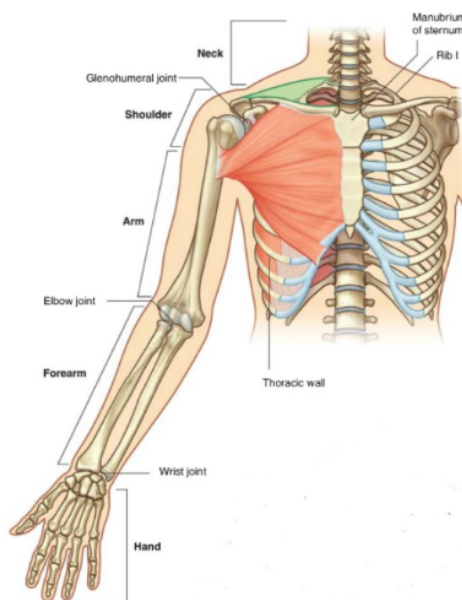
Figure 2.1: Anatomy of the upper limb, anterior view. Adapted from Drake et.al. 2015[19].

2.1.1   Hand architecture

The human hand's interior structure includes a variety of bones, muscles, nerves, veins, and arteries, allows for the precise execution of movements. The human hand comprises the wrist, palm, and five fingers. The thumb and the four fingers of the hand make up most of the hand's function[21]. The brain hemisphere on the opposite side of the body controls each hand, which is made up of 27 bones with four fingers (Index, Middle, Ring, and Little) and a thumb[22]. As shown in Figure 2.2 each hand is divided into three groups: the carpal bones, the metacarpal bones, and the phalanges. It has 25 joints (despising the carpal and metacarpal joints in the base of the palm), with a total of 25 degrees of freedom (DoF) which allows different hand movements for the 31 muscles that are made up[23].
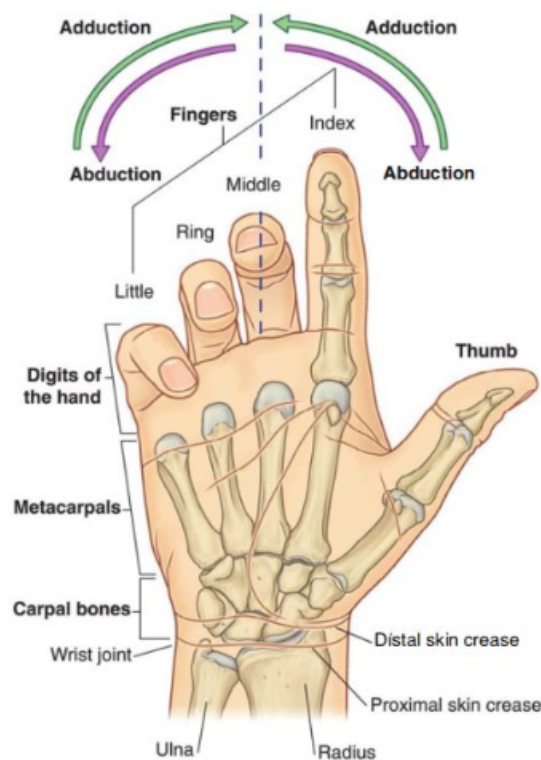
Figure 2.2: Human hand architecture. Adapted from Drake et.al. 2015[19].

Carpal bones

The carpals are a collection of bones that make up the wrist of the hand. They are responsible for the wrist's back-and-forth motion. It articulates directly with the radius, indirectly with the ulna, and below with the five metacarpals (as shown in Figure 2.2 and more in detail in Figure 2.3). This group of bones aid in the stability and movement of the wrist about the frontal or coronal plane and the sagittal plane[24]. The eight carpal bones are small, allow only limited movement, and are separated into two rows overlaid on top of one another. As a result, the bones work together as a unit. The proximal row connects to the forearm and articulates with the distal ends of the radius and ulna, where the scaphoid, lunate, and

triquetrum bones are located, and pisiform when arranged on the palm. Also, the trapezium, trapezoid, ample bone, and hamate bone make up the distal row of bones[25].

Metacarpal bones

The hand's wrist, palmar and dorsal regions are formed by these metacarpal bones, which also constitute the intermediate portion of the fingers. The metacarpals that form the palm are five long bones numbered from 1 to 5. In Figure 2.3, adapted from Tang and Varcallo[26], are shown the five metacarpals related to one digit: Metacarpal I is related to the thumb, and Metacarpals from II to V are related to the index, middle, ring, and little fingers, respectively[19]. Moreover, each metacarpal consists of a base, a shaft (body), and, distally, a head. The heads form the knuckles on the dorsal surface of the hand when the dingers are flexed here a metacarpals articulate with the proximal phalanges of the fingers; in addition, the bases of the metacarpal bones of the fingers articulate with each other[24].

Phalanges

Phalanges are small bones that make up the fingers. Each finger consists of three phalanges with similar morphology: the proximal phalanx, the middle phalanx, and finally, the furthest from the hand, the distal phalanx. Except for the thumb, there are only two phalanges: distal and proximal, due to their position relative to the hand[19] (as can be seen in Figure 2.3). Each phalanx has a base, a shaft (body), and distally a head. Each proximal phalanx's base articulates with the corresponding metacarpal bone's head. Additionally, the head of each distal phalanx, which is located beneath the palmar pad at the end of the digit, is nonarticular and flattened into a crescent-shaped palmar tuberosity[27].

2.1.2 Joints of hand

The bony structure of the hand consists of an adjacent joint between two bones, whose proximity dictates whether the wrist and finger joints may move[21]. The ligaments' connection to the hand's bones enables them to support the joints and restrict the bones' range of motion[28]. Each bone has articular surfaces coated in cartilage, allowing the hand's internal structure to be maintained. Finger joints result in variable DoF at each joint. The hand movements are attributed to the thumb orientation, specific to the carpometacarpal joint (CMC), resulting in increased flexibility and a wide range of movement[29]. At rest, the MCP joint flexes 45°, the PIP joint flexes 30° to 45°, and the DIP joint flexes 10° to 20°. When the hand is extended, the reference angles vary significantly between individuals. For instance: for the MCP joint, the thumb is flexed at 90°, and the other fingers move around 70°, while the PIP and DIP joints are extended flexes between 110° and 90° DIP, respectively. The joints vary depending on the bones that are joined, as can be seen in Figure 2.4 (adapted from Bullock et.al[30]) seven types of joints are included the same ones that are studied in detail below:

Carpometacarpal Joint (CMC Joint)

The carpometacarpal joint facilitates pressure and movement in three planes with only two control axes. It creates a single synovial cavity by joining the mid-carpal cavity and the trapezoid. Their anatomy allows humans the ability to thumb opposition with a stable pinch. Also, the first metacarpal joint is referred
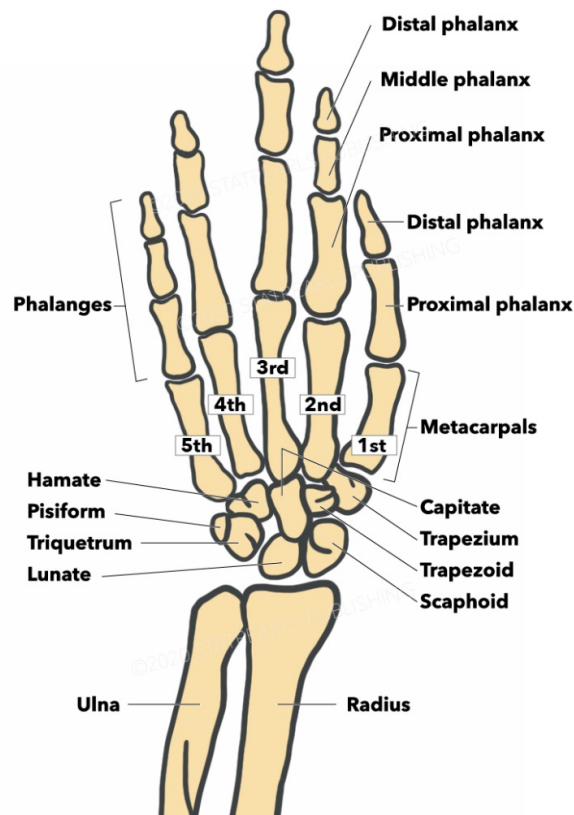
Figure 2.3: Carpals, Metacarpals and Phalanges of the human hand. Adapted from Tang and Varcallo, 2021 [26].

to as the trapeziometacarpal joint or thumb joint, and it is thought to be the unique joint in the upper limb [31]. The trapeziometacarpal gives it a concave shape in the transverse direction but a convex shape in the anteroposterior direction where the first metacarpal is located, allowing the thumb free movement and flexing considerably in a tight grasp. Then, it enables the finger to flexion/extension, abduction/adduction, and opposition or circumduction [27].

The carpal joints of the last four fingers are flat, allowing sliding motion except for the first metacarpal. The mobility between the carpal bones is entirely restricted, while intrinsic ligaments support the intercarpal joints [31]. Interosseous ligaments connect the base of the metacarpals to the carpal bones. Moreover, there are inter-skeletal ligaments, palmar, and dorsal in the second, third, fourth, and fifth metacarpal fingers [21]. On the other hand, the scaphoid is a biomechanically significant carpal bone because it spans both proximal and distal carpal rows allowing stability of the mid-carpal joint during wrist movement [31].

Trapeziometacarpal Joint (TM Joint)

The trapeziometacarpal (TM) or first carpometacarpal (CMC), or basal thrumb joint is a biconcave-convex saddle joint that is composed of the first metacarpal bone (1st MC) and the trapezium [32]. According to biomechanics, TM is essential because it provides the thumb with an extensive range of motion, such as

abduction/adduction, flexion/extension and opposition[33]. In order to do this, the thumb rests at the TM joint, pronated and flexed by around 80 degrees concerning the plane of the other metacarpals, resulting in the opposition of the thumb[34] .

Intermetacarpal Joint (IMC Joint)

The human hand can assemble all five fingers at once thanks to the intermetacarpal (IMC) joints connecting the neighbouring metacarpal bones. This increases the area where precision gripping is feasible (for two- and three-finger pinch)[35]. In the second, third, fourth, and fifth metacarpal, some ligaments unite them, and some spaces called arthrodias allow the bones to be articulated between them. The ligaments that reach the joint capsule are the interosseous metacarpal ligaments[27]. Anteriorly are the palmar metacarpal ligaments, and posteriorly are the dorsal metacarpal ligaments.

Metacarpophalangeal Joint (MCP Joint)

The metacarpophalangeal (MCP) joints are formed by connecting phalanges to the metacarpals; they form part of the palm, the most distal part. It is a condyle-shaped joint that allows biaxial movements in two axes to do flexion-extension and abduction-adduction[19]. In addition, ligaments connect each metacarpophalangeal joint, the internal lateral ligaments (towards the fifth finger) and the external lateral ligament (towards the thumb). Similarly, the intermetacarpal or the transverse ligament of the metacarpal fixes the joint and gives stability, connected to the second to the fifth metacarpophalangeal joint[21]. Also, this joint presents the sesamoid bones in the first metacarpophalangeal joint, where some muscles can be inserted.

Distal Interphalangeal Joint (DIP Joint)

The distal interphalangeal (DIP) are hinge-type joints. They are biaxial joints, and since movement occurs in the sagittal plane, they can only flex the finger. In addition, the DIP joint has a single fixed transverse axis, passing through the center of curvature of the condyle of the phalangeal head, where flexion/extension movements occur over a range of 90 degrees[34], as shown in Figure 2.4. There are two interphalangeal joints: the proximal joints, which always connect the proximal phalanges, and the middle phalangeal joints, which connect the middle and distal phalanges[21]. The thumb has only one interphalangeal joint; the interphalangeal joints have internal and external ligaments that reinforce the joint[25].

2.1.3 Muscles of Hand

The nervous system controls the muscle, which connects to and helps support the skeletal system. Muscles consist of muscle fibers containing sarcomeres, which are smaller repeating units in the muscle. Through a series of complex events, sarcomeres are responsible for contraction and relaxation, allowing for a variety of rapid movements and finer movements[36]. The muscles of the hand and wrist lie in the forearm, and narrowing at the tendons traverse the wrist to reach attachments to the bony or ligamentous components of the hand[27]. The muscles of the hand are made up of extrinsic and intrinsic muscles.
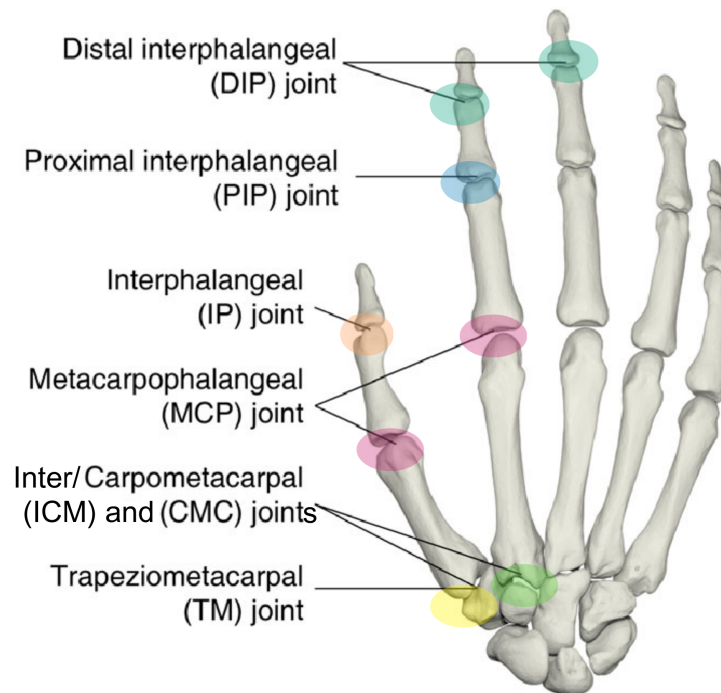
Figure 2.4: Joints of the right hand, dorsal view. Adapted from Bullock et.al. 2012[30].

Extrinsic Muscles

The extrinsic muscles of the hand originate in the forearm with a long tendon which inserts on the dorsal part of the hand, that is, on the metacarpals[27]. Therefore, these muscles allow us to grasp movements and provide thumb motion and stability[34]. In addition, the intrinsic muscles are found distal to the wrist joint and inserted into the extensor mechanism or the fingers allowing fine, precision movements between the fingers and thumb, complementing the extensor and flexor muscles of the forearm[37].

Intrinsic Muscles

The most superficial intrinsic muscles have mobile functions; these are the muscles of the thenar eminence, which are attached to the thumb and work simultaneously on the TM, MP and IP joints. Moreover, the muscles of the hypothenar eminence are attached to the little finger[34]. In contrast, the deeper intrinsic muscles branch the ulnar nerve except for the three thenars and two lateral lumbrical muscles because these muscles are innervated by the median nerve[19]. The flexor muscles, which run on the anterior part of the forearm, and the extensor muscles, which originate from the lateral epicondyle and parts of the ulna, run down the dorsal side of the forearm, aiding in pronation of the hand. These two muscles allow the bending of the wrist to move the hand and fingers[27].

2.1.4 Nerves of the hand

The hand contains many specialized structures, which work synchronously, providing precise motor biomechanics and fine tactile senses [27]. Sensory and motor function of the hand depends on the median, radial, and ulnar nerves, which provide the hand with the sensation of touch, pressure, pain and temperature, as shown in Figure 2.5 (obtained from Maw et.al [27]). These nerves run from the underarm and various locations in the arm and forearm until they reach the wrist. From there, each nerve will be distributed throughout the hand through motor neurons and sensory neurons until it reaches each finger [38].
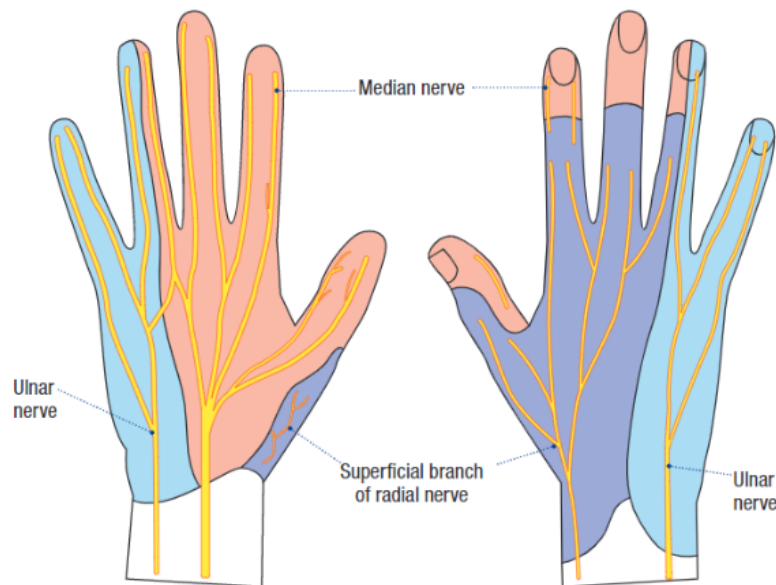
Figure 2.5: Sensory nerve distribution of the hand. Adapted from Maw et.al. 2016 [27].

2.2 Movements of the Hand

Grasping and manipulating objects is one of the main functions of the hand. So, the proper functioning of the hand depends on its ability to rotate, that is, its location and orientation. The rotation of the hand will be possible due to the rotation of the entire upper extremity of the shoulder and also to the rotation of the forearm that allows pointing the palm upwards or supination and downwards or pronation [39]. The forearm and hand consist of the cubitocarpal and the radiocarpal joint, allowing the hand's radial and ulnar flexion and extension. In addition, the wrist joint has two degrees of freedom of movement. In contrast, the thumb has different mobility than the other four fingers [21].

2.2.1   Pronation and supination

Pronation and supination of the hand have been developed gradually due to increased mobility of the rotation of the radius at the elbow and movement of the distal end of the radius over the ulna[19]. These movements occur in the forearm and are possible because it involves supinate and pronate muscles. Pronation describes a rotational movement of the forearm resulting in the hand from the palm facing posterior when it is in an anatomical position. While supination brings the anterior palm position (upwards), as shown in Figure 2.6 obtained from Mansfield and Neumann[40].
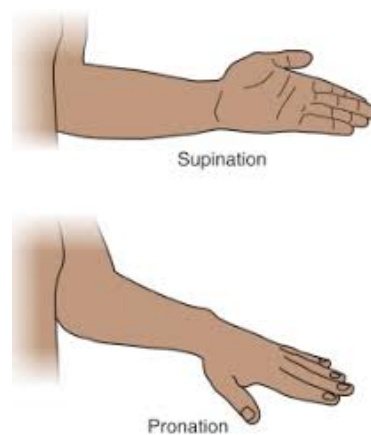
Figure 2.6: Pronation and supination of the hand. Adapted from Mansfield and Neumann, 2019[40].

2.2.2   Flexion, extension, abduction and adduction movements of the hand and fingers

The localization of the main joints and bones that make up the upper extremities: shoulders, arms, and forearms, place the hands in different positions relative to the body. The wrist's carpal bones thus perform movements of flexion, extension, abduction and adduction as can be seen in Figure 2.7 in (a) and (b) respectively. On the other hand, in the resting position, the fingers form a flexed arch, but anatomically, the fingers are extended, and the thumb is rotated 90 degrees concerning the other four fingers. Abduction and adduction of the fingers are performed about an axis that passes through the center of the middle finger in its anatomical position[19].

The thumb is positioned at right angles to the orientation of the other fingers (index, middle, ring, and little). Consequently, the thumb movements occur at right angles to those of the other digits. For instance, the thumb is brought to the palm during flexion, while the extension occurs at 30 or 40 degrees as can be seen in Figure 2.8 in (a) and (b) respectively. However, when the fingers are hyper-extension, they can reach up to 90 degrees[40]. At abduction, the thumb is separated from the other fingers (Figure 2.8 (c)). Moreover, thumb opposition occurs when there is a rotation of the Metacarpal I in the wrist, moving the thumb in front of the other fingers[19] as shown in Figure 2.8 (d).
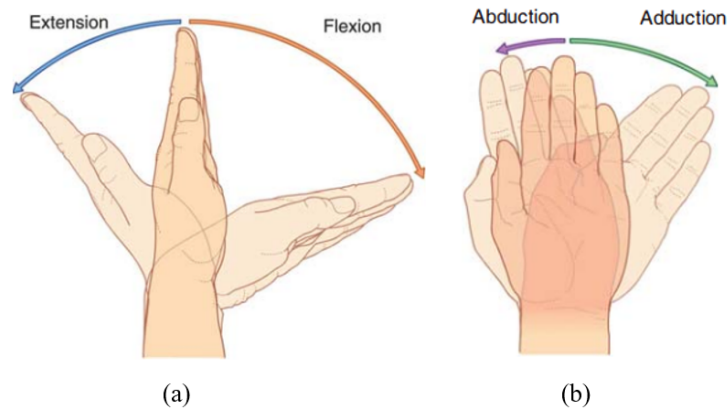
Figure 2.7: Hand movement about the wrist joint: (a) extension and flexion movement can be seen on the left and (b) abduction and abduction movement is on the right. Adapted from Drake et.al. 2015[19].
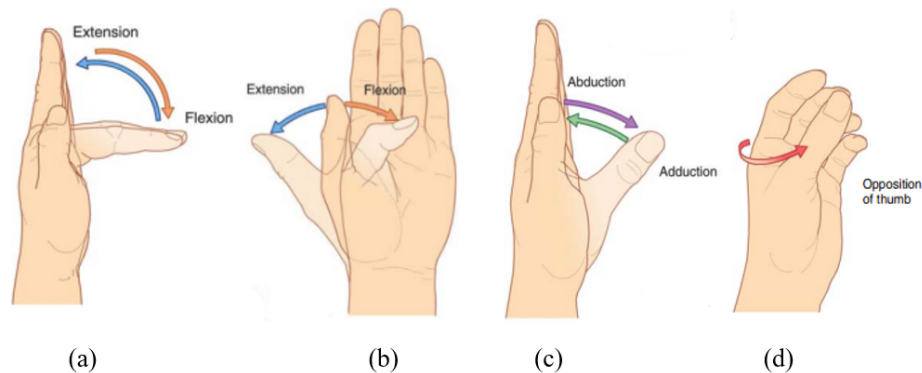
Figure 2.8: Thumb motions: (a) flexion and extension of fingers (middle and ring), (b) flexion and extension of the thumb, (c) abduction and adduction of the thumb, (d) opposition of the thumb. Adapted from Drake et.al. 2015[19].

2.3 Human Hand Grasps

Hand muscles and joints enable various movements for successfully grasping and manipulating objects in different acceptable positions between the human hand and the object[41]. Most studies are based on hand movements' taxonomy, which includes a division between power and precision tasks[42]. Among them are grasping motions, which refer to movements carried out by force exerted by the fingers on the object at the time of this being grasped, and that it can be kept totally or partially inside the hand[43]. This way, the gripping force is continuously adjusted when lifting or carrying objects. The human hand has 15 joints, not including the carpal and metacarpal joints of the palm[23].

On the other hand, recent research indicates that during the pressure grasping task, the index finger and thumb are the main fingers that exert this gripping force[44]. Human hand grasps are distinguished by the precision or force required to perform them accurately. Movements performed by the human hand

include spherical grip, palmar grip, cylindrical grip, lateral grip and hook grip[41] as shown in Figure 2.9 the different hand movements when grasping an object.
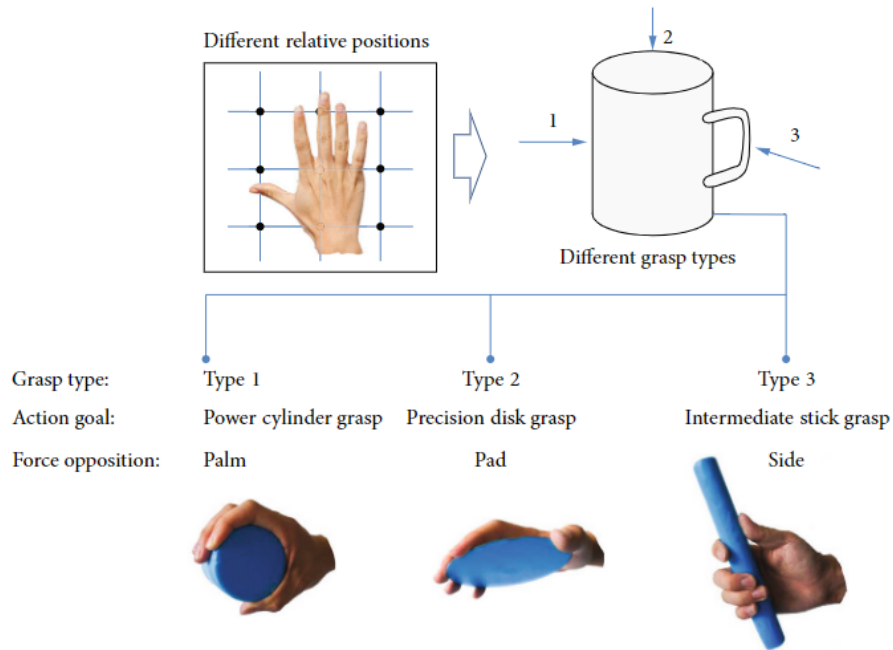
Figure 2.9: Example of grasping tasks include a power cylinder, precision disk and intermediate stick grasps with their respective hand positions. Adapted from Liu et.al. 2015[41].

Moreover, in the study of current prehensile taxonomies of the human hand, is important to consider three categories: power, intermediate, and precision, which have subdivision according to the position of the abducted or adduced thumb (as can be seen in (d) of Figure 2.10) concerning the other four fingers[23]. Depending on the number of digits involved, these functional units form a virtual digit (VF) during manipulation, as shown in Figure 2.10, which is determined by the applied force's direction[42].
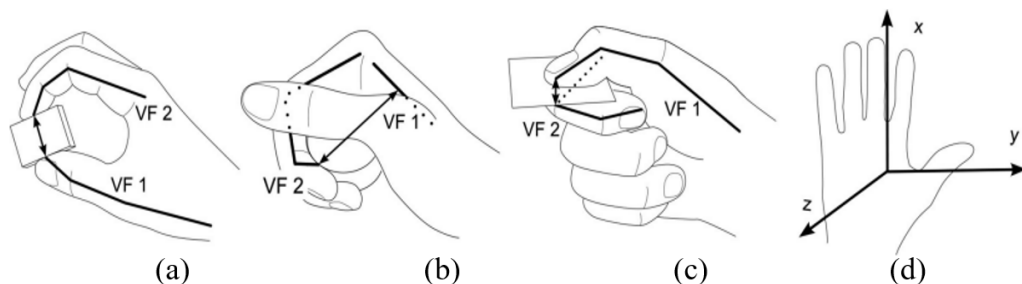
Figure 2.10: Opposition types of the grasping hand: (a) Palmar Pinch or parallel to the palm, (b) Medium Wrap or perpendicular to the palm, (c) Lateral or transverse to the palm, (d) Hand coordinate system. Adapted from Feix et.al. 2015[23].

Then, grasping objects will be possible thanks to the four fingers and the thumb's ability to be placed in front of the fingers, which means that hands in this position can grasp larger objects, such as stones or heavy bottles[45].

2.4 Biomechanical Hand Analysis

Hand biomechanics allows an understanding of the correct functioning of the hand. By studying the structures involved, such as bones, muscles, tendons, and ligaments that form a complex structure, it is possible to understand the biomechanical motions that allow the hand to function effectively and how patients used it before their injury[46]. Hands perform a variety of functions for daily activities. In consequence, the physical capacity of the hand has been evaluated by biomechanical methodologies. Biomechanical analysis of the human hand is covered in (1) anthropometry, (2) kinematics, (3) kinetics, and (4) electromyography (EMG)[47].

Hand Anthropometry is the basis of biomechanical analysis[47]. It allow to acquire the anatomical measurements of the hand, such as size, shape, and range of motion (ROM), which are usually used to design rehabilitation hand products and to ensure safely use[48].

According to Laprensa et.al, mentioned that kinematic analysis of the human hand is essential to evaluate functional alterations as a result of traumatic or neurological events, as well as its ability to grasp and manipulate objects. Kinematic analysis is also essential for reproducing the hand's kinematic structure as faithfully as possible[49]. The most commonly used technique for measuring kinematic variables such as trajectory, angle, velocity, and acceleration is the three-dimensional (3D) motion analysis system. An analysis of this system requires the use of marker sets and kinematic models[47].

Rehabilitation devices are designed and controlled based on the dynamic properties of joints of the upper limbs. Serbest et al. have suggested that mathematical techniques and some simulation models can be used to analyze the hand's movement because they provide specific information that can help a researcher design an experiment design[50]. Consequently, a kinetic hand model is used for analyzing the internal load (force and moment) in muscles and tendons during static or dynamic movements[47].

Furthermore, electromyography is a specialized diagnostic technique that analyses electrical signals generated by skeletal muscles[51]. An EMG can provide a valuable tool by detecting and classifying movements in the human body in a natural way. As a result, biomechanical analysis of body movement, medical abnormalities, physiotherapy, biofeedback, ergonomics research, rehabilitation, sports medicine and training can be performed using these signals[52]. In order to perform an accurate analysis, it is essential to understand how to use the EMG equipment, where to place the electrodes, where the muscles are positioned, and how to acquire and process the signals[47].

2.5 Myoelectric Signals

The myoelectric hand is a type of prosthesis focused on recovering motor functions lost due to amputation or degenerative disease of an upper limb. Control assistive devices for amputees are based on using myoelectric signals (MES) because this signal is an electrical potential generated by the skeletal muscles; as a result, it allows an increase in the capacity movement of the prosthesis when used by the user [29], [53], [54].

Electromyography (EMG) is a biomedical signal obtained from the electrical stimulus of the nerves generated in the Central Nervous System. (CNS), therefore, EMG is used to read myoelectric signals, which are monitored by two techniques. The first is a needle electrode, an invasive method inserted inside the muscle, and the second is a surface electrode, a non-invasive method using a surface electrode sensor. This method has been used in several applications because it shows essential information about the signal acquisition [51]. In addition to providing information about neuromuscular diseases, EMG signals can be used to diagnose injuries to any body muscle. When EMG signals are monitored, it is possible to identify myocardial and muscle failures as well as characterize a user's intention of movement[55]. Therefore, patients who use myoelectric prostheses for upper limb rehabilitation may restore activities of daily living without needing help from someone and reduce the possibility of overuse and secondary injuries; as a result, it will mimic the natural movement of the human.

Figure 2.11 shows characteristics of EMG signals, first observed in a time domain as a record of what happened to the signal as a function of time. As a result, the amplitude is the difference between the maximum negative peak and the maximum positive peak during the motor unit potential (MUP) generated by muscle fiber. Additionally, duration refers to the interval between the first and last waves that exceed a predefined amplitude threshold. The baseline reaches an absolute value of amplitude broader than 0.02 mV. Moreover, EMG signals cover the range from 5 Hz to 2 kHz[51].
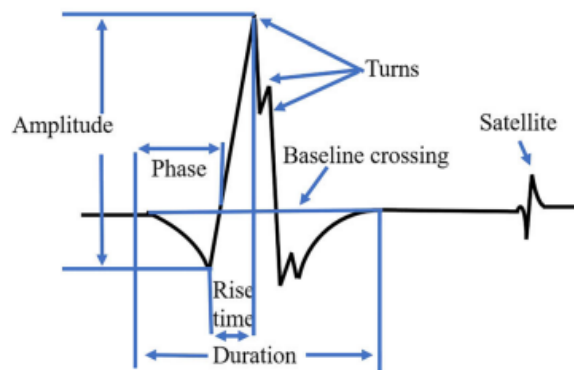
Figure 2.11: Characteristics of EMG signal. Adapted from Mehendale et.al. 2020[51].

2.5.1   EMG signal acquisition and processing

An EMG signal acquisition system consists of four main stages: (1) signal collection, (2) signal amplification, (3) signal filtering, and (4) analog-to-digital converting. Depending on its operational characteristics, each stage has specific requirements[56]. All steps are essential for analyzing and interpreting myoelectric signals (MES) as shown in a Figure 2.12.

Myoelectric signals from muscles are extracted using sensors. Electrodes measure the level of activity by recording the electrical activity within them. Also, muscular constraction's amplitude in voltage can vary from $0\mu V$ to 10mV. Since many other biosignals may be present around the muscle, electrode placement is essential to achieve an adequate signal-to-noise ratio (SNR).
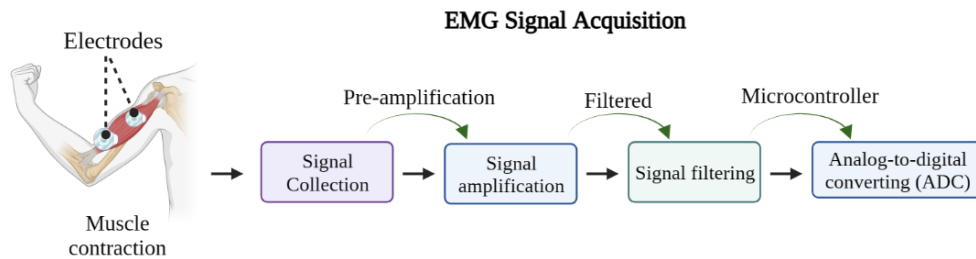
Figure 2.12: Block diagram of EMG signal acquisition. Adapted from Rodríguez-Tapia et.al. 2020[56].

Hence, the filtering stage's design significantly impacts the quality of EMG signals. The data is then fed into an analog-to-digital converter (ADC). Advanced signal processing methods must process EMG signals. As a result, it is necessary to design the analog-to-digital conversion stage carefully. As part of the design of the ADC stage, three main variables must be taken into account: the open-loop gain used during the amplification stage, the maximum output voltage at the system's back-end for acquiring EMG signals, as well as additive noise. Additionally, it is necessary to determine the optimal sampling frequency for the ADC stage, which is another important design parameter[55],[56].

Physiological control signals acquired by sensors can be used to determine the user's intent for controlling the hand prosthesis. Surface electrodes on prosthetic hands are 0.5-2.5 cm wide and non-invasive because they are positioned on the surface, as shown in Figure 2.13. Moreover, there are two surface electrode types: gelled EMG electrodes and dry EMG electrodes. By electrolytic conduction, surface electrodes detect changes in the surface of the muscle and the body's skin based on the principle of chemical equilibrium[54],[51]. The literature has recommended that a first electrode be placed on the Flexor Digitorum Superficialis (FDS) muscle to assess gross finger flexion and grasping skills, and a second electrode should be placed on the Extensor Digitorum Communis (EDC) muscle to assess gross finger extension and opening skills[29].
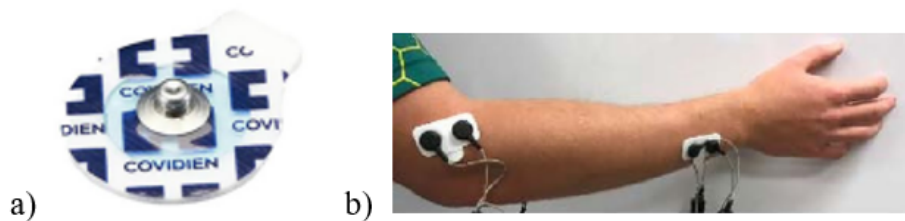
Figure 2.13: EMG sensor: (a) Surface electrode, and (b) the location of the two electrodes that acquire the signal adapted from Mehendale et.al. 2020[51] and Rodríguez-Tapia et.al. 2020[56].

An upper limb prosthesis is usually controlled by a surface electromyography (sEMG) signal generated from the residual limb or the accessory muscles of the amputated limb. When electrodes are in contact with the skin, they allow the user to take control of the myoelectric prosthesis to open or close the hand and control an artificial wrist rotation and individual finger articulation. On the other hand, accurate

measurement of sEMG signal acquisition depends on the type and placement of electrodes on the muscle. Also, skin preparation is essential for helping to maximize the noise of the environment because it affects signal processing[57].

2.6   Design requirements for a myoelectric prosthetic hand

The principle of operation of a hand myoelectric prosthesis principally may vary depending on the functions needed by the patient. There are a number of requirements for each function that must be taken into account to conduct an effective search for solutions. Among the fundamental requirements for the manufacture of a myoelectric prosthesis are detailed below, in Table 2.1.

Table 2.1: Functions of design with the requirements for a prosthetic hand.

Aspect	Parameter	Requirement
Prosthetic hand	Manufacturing Availability	Partly 3D printable Open source
Actuation	Output force, Size and Moving speed	30 N of pinch force, To fit inside the prosthesis, >172 degrees/s
Control system	Connectivity Size	Compatible with electrodes and actuation Able to fit inside the prosthesis
EMG measurement	Applying of electrodes	Multiple use, non-irritating, non-invasive
EMG analysis	Number of variables Computational load	Control of all DoF of prosthetic Be able to run on selected microcontroller
Power source	Supply MCU	+ 5V connection
Costs	Material costs	<180 dollars
Weight		<400 g

According several researchers, for the prototype of the prosthetic hand it is better if 3D printing is applied, so that it is easier to adapt to the needs of the patient and it allows for local manufacturing in developing countries[58]. As is known, this type of prosthesis requires actuation to be able to move the hand. According to several studies it has been determined that the output force of a prosthetic hand must be able to reach a pinch force of 30 N which is the minimum amount required to perform activities of daily living[59].

In spite of the fact that grasping speed of a normal human hand is approximately 2290° per second[60], the required minimum speed for daily life activities is much lower. According to Heckathorne, in addition to having the appropriate measures to be placed inside the prosthesis, for pick and place tasks as well as to grasping objects it must have a speed of at least 172° per second as part the design requirement for the actuation mechanism[60]. In this way, depending on the degrees of freedom (DoF) that the prosthetic hand offers and if there is enough space more actuators will be implemented.

Furthermore, a control system is needed for the activation of the actuator and the analysis of the EMG signal. In general microcontrollers (MCU's) integrated in a printed circuit board (PCB) are used for this

purpose. In order to prevent any damage is necessary the implementation of the MCU inside the prosthetic hand as a result a reduced size is required. The algorithm applied to execute the analysis of the EMG signals will be performed from the MCU, this requires that the computational load of the algorithm is properly adjusted to the computational capacity of the MCU[9].

Besides, in a myoelectric prosthesis the technique applied for measuring muscle activation is the electromyography (EMG). The patient will have control over the prosthesis through electrodes that detect muscle activation signals[54]. Electrodes, generally attached to the skin or implanted close to a muscle, measure the difference in electrical potential on the skin at two proximal points[61]. For comfortable use of the prosthesis, the electrodes should be safe to use, avoid irritations or hurt the skin. It need to be easy to apply and detach as well as able to run effectively for multiple use[54].

For the analysis of EMG signals it is necessary to take into account the number of variables that can control all the degrees of freedom that the system has as well as the compatibility with the selected microcontroller. The signal that the electrodes detect is measured, rectified, amplified, filtered, sampled, and used for further analysis in relation to the study of EMG signals.[62]. There are several algorithms that can be applied for analysis. The number of degrees of freedom that can be regulated varies between algorithms. The prosthetic hand used for this investigation will determine how many degrees of freedom it has[61].

In relation to the power source this must be sufficient for the entire system to supply the PCB and the actuation mechanism. Depending on the type of actuation, the power source may require an additional source of power to supply the actuation mechanism in addition to having to be electric for the control unit. Also, for a prosthetic hand it is necessary to consider the power source's replacement or charging. In general, more than 5 V connection is needed.

The typical human hand weighs approximately 400 g, as a result the weight requirement for the prosthesis is set at 400 g for patient's comfort. Since the power source won't be built into the hand, it can be worn on another part of the body. In this regard, the weight of the battery will not be taken into account when designing the weight of the prosthesis[63].

Last but not least, the material costs of the prosthesis should be adjusted to a value less than 226 dollars to make it easily accessible[64]. The goal of this project is to create a prosthesis that is cheap, even in lower income countries. Middle low and middle income countries are defined as countries with a GDP per capita of 2,572.7 USD and 5,494.4 USD by the World Bank Group[65]. One of the countries with worlds largest population is India (1.4 billion)[66], a lower middle income country with an average annual income per capita of 2,256.6 USD[65]. The prosthesis to be designed in this project will have a maximum cost need of 10% of the typical monthly income in India, or a cost of no more than 226 USD. For Ecuador, this value is aacesible since the value according to 2021 data is adjusted to a GDP per capita of 5,965.1 USD[67].

2.7 Hand Prosthesis Research

The artificial hand is based on the human hand's anatomy, which is a complex organ that plays a crucial role in grasping objects. Nowadays, more sophisticated devices to mimic the hand's natural movement are on the market. The most common prosthetic hands are passive and consist of a static or adjustable prosthesis[68]; they offer a lifelike appearance and are used for various activities. Static prostheses cannot be moved at all. Meanwhile, adjustable prostheses feature an adjustable grasping mechanism in multiple orientations[69].

Moreover, power prosthetic hands are classified as body-powered, a mechanism by which the human body moves through wires. Although it is lightweight, one of its disadvantages is that the user may not be able to grasp objects accurately. And external powered prosthetic hands have based on actuators and external power, such as some prosthetic hands controlled by an EMG for achieving high locomotion detection[70]. On the other hand, hybrid prostheses are multi-articulated devices used for a user who loses an upper limb. It is an entirely mechanical design controlled by EMG. These devices are robust and provide different hand motions but depend on the actuator system[68,71].

Despite the high accuracy of EMG signals, researchers are currently exploring the best ways to combine EMG with other systems, such as artificial intelligent and augmented reality (AR)[72], a tongue control system[73], and so on. The following section presents the characteristics of commercial upper limb prostheses available in the market.

2.7.1   Commercial prosthetic hands

Exoskeletons have been studied and developed during the last years to simulate human hand movements and provide adequate rehabilitation for people with prostheses. However, these handheld exoskeletons still face many challenges that may include the proper study of hand biomechanics, ergonomics[11], human-robot physical interactions, the use of sensors, and cost, among others. According to the literature, many studies on developing upper limb prostheses are based on a complex hand structure to enable various movements[29]. Therefore, in 1922, Jacob Hüfner invented a hand with a lock mechanism that could be activated before or during grip, making it easy to operate, as shown in Figure 2.14. "Hüfner hand" was used as the prototype of the first myoelectrical controlled hand described by Reinhold Reiter in 1948[4].

Commercial upper limb prostheses available in the market have become more sophisticated. Because robotic hand prostheses are composed of electronic and mechanical parts fitted with sensors and actuators, the hand can adapt to the object's geometry and perform different grasping movements. The following section describes some features of the development of a prosthetic hand in which surface electromyography (sEMG) signal is used for grasping objects: (1) Vincent Hand Evolution 4, (2) Michelangelo Hand Transcarpal, (3) Bebionic Hand, and (4) i-Limb® Quantum Bionic Hand.

Vincent Hand Evolution 4

Vincent Evolution 4, as can be illustrated in Figure 2.15 is a new generation of hand prostheses with a unique design and weighs approximately 390 grams. The prosthesis is uncompromisingly waterproof and has gel fingers that permit greater flexibility when the hand prosthesis performs the movements[74]. It consists of a control system with four channels that allow up to connected four EMG sensors on the hand. Additionally, it offers different grips such as flat hand, cup holder, clamp grasp, power grasp, and lateral grasp / lateral thumb[75].
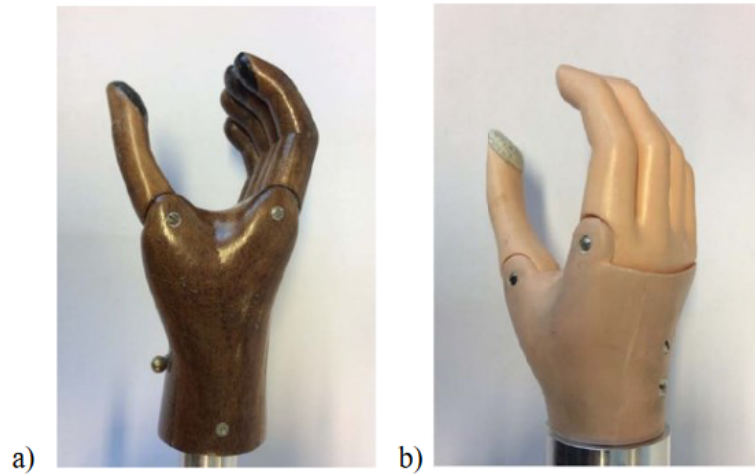
Figure 2.14: a) Original "Hüfner hand" made of wood, b) at the end of the 20th century, the plastic model of the "Hüfner hand" was created. This prosthesis has a locking mechanism that can be seen in the palm. Adapted from Smit et.al. 2020[4].

Figure 2.15: Vincent Hand Evolution 4. Adapted from Vincent Systems, 2020[75].

Michelangelo Hand Transcarpal

Michelangelo Hand, shown in Figure 2.16, developed by Otto Bock, is a fully articulated robotic hand prosthesis with seven grip patterns[76]. Through muscle signals, the user controls the speed and force of the grip, which is similar to and feels like a natural hand. Michelangelo's Hand weighs 510 grams, resulting in a maximum grip force of 70 newtons[77]. Also, a powered thumb and four movable fingers can be controlled separately with muscle signals[78].

Figure 2.16: Michelangelo Hand adapted from Williams, 2021[76].

Bebionic Hand

Bebionic Hand, developed by Otto Bock, is a bionic hand controlled via a direct myoelectric system. In order to detect a muscle movement, myoelectric sensors are placed on the residual limb's skin. Due to its weight of 500 grams and the ability to generate 140 newtons of force, the Bebionic Hand can perform light to medium tasks. It has five independent linear actuators that work at five speeds with force motors[79]. In addition, it does not offer any form of sensory feedback and has 14 grips available, divided into primary and secondary grips[80], shown in Figure 2.17. Bebionic wrist allows upward rotation of the palm at 180 degrees, an internal rotation of 50 degrees, and flexion and extension movements at 30 degrees[81].

Figure 2.17: Bebionic Hand adapted from Williams, 2021[81].

i-Limb® Quantum Bionic Hand

Össur Company developed i-Limb hand, offering 12 different grips. They are not finding evidence that the control system is superior to other bionic hands. I-Limb employs several innovative features to augment user control. All bionic hands offer a method of rotating through available grips. Repeated open gestures are one common way of doing this, but this is impractical when so many available grips exist. For this reason, a few bionic hands offer natural grip selection through specific gestures or the ability to change

grips using a mobile application[82]. The i-Limb as can be seen in Figure 2.18 offers all possible forms of grip selection: rotation through grips via muscle triggers; natural grip selection through specific gestures; selection via a mobile application; proximity control via grip chips[83].

Figure 2.18: i-Limb® Quantum Bionic Hand adapted from Össur Company, 2020[83].

Below, Table 2.2 presents a summary of essential features for before mentioned commercial bionic prosthetic hands which are controlled by EMG signals.

Table 2.2: Summary of commercial bionic prosthetic hands characteristics. Adapted from Dunai et.al. 2021[79] and Mochammad et.al. 2016[84].

Characteristics	Vincent Hand[75]	Michelangelo Hand[76]	Bebionic Hand[80]	i-Limb® Hand[82]
Developer	Vincent Systems	Otto Bock	Otto Bock	Touch Bionics
Weight (g)	390	510	500	599
Operating voltage (V)	6-8	11.1	7.4	7.4
Battery type	li-Pol	li-ion	li-ion	Lithium polymer
Electric current (mAh)	1300-2600	1500	1300-2200	1300-2400
N° Actuators	6	2	5	6
Type of actuators	DC motor worm gear	-	DC motor head screw	DC motor with worm gear
Active fingers	5	3	5	5
Number of joints	11	6	11	11
Degrees of Freedom	6	2	6	6
Force (N)	60	70	140	100
Force transmission	Gears	Gears	Gears	Worm Gears
Movement command	Single trigger EMG	Switching	Co-contractions	Double and triple impulse
Movement control	Single trigger EMG	EMG, 4 channels	Sequential EMG	Mobile app, EMG
Sensory feedback	Vibrations	No	Audible bip vibrations	No

Chapter 3

Methodology

This section presents a descriptive summary of the methodology carried out in this study. Thus, it provides information about the features of the myoelectric hand prosthesis prototype for people who have suffered a hand amputation. The different parameters and requirements for the structural design of the prototype are based on upper limb prostheses commercially available. Each adopted alternative will use existing technologies, in line with the purpose of manufacturing and use in developing countries with limited resources. The process carried out for constructing a prosthesis is described in detail in the next sections. The main phases are shown in the flowchart of Figure 3.1. First, the hand anthropometric specifications selected according to the active motion range of fingers described in DIN 33.402 standard measurements for the human hand are presented. Then, in order to generate solutions based on user suggestions in conjunction with the engineering bases, is described the generalities of the criterion of Concurrent Engineering (CE) applied to determine the best material for prototype design. Afterwards, is describes the Structural Design followed for the palm and phalanx designs as well as the 3D model assembly. Next, in section 3.4 are defined the desired movements of precision open, cylindric and tip grips for the prosthetic hand. In the last sections, are described more in detail the electronic components used for actuation, control system and power source. Next, in terms of EMG signals also are presented the alternatives applied for the measurement and analysis of detected signals. Finally, the applied parameters as well as the experimental setup for the static analysis are explained.
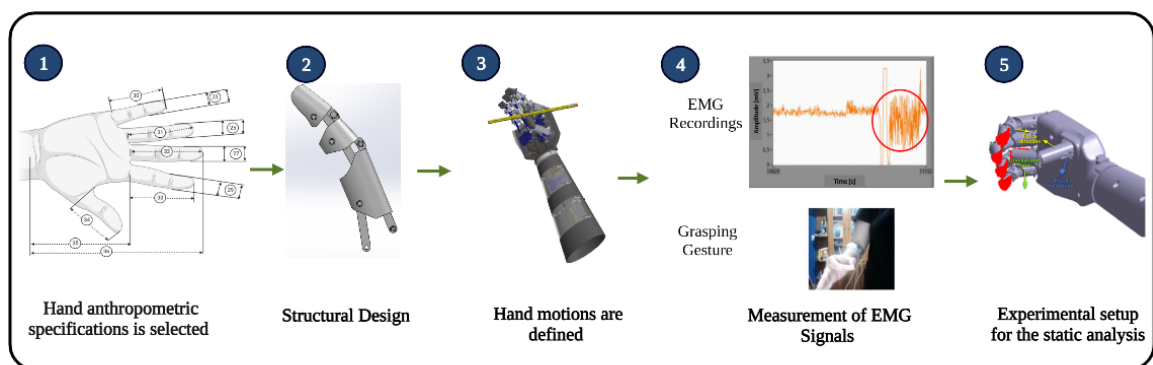

Figure 3.1: Block diagram for the methodology carried out for the design of a prototype of myoelectric hand prosthesis.

3.1   Hand Antropometric specifications

The measurements of the human body, both at rest and in motion, are determined by the length of its bones, muscle mass, tissues, and joints. Thus, the dimensions differ between the sexes (male and female) and between individuals within a group. In Ecuador, there still needs to be a record of anthropometric measurements of the human body. Therefore, the human body's measurements follow the DIN 33.402 Standard. The anthropometric measurements presented in DIN 33.402 Standard are a compilation of different studies carried out by different countries, among which are: Germany, England, France, Sweden, Switzerland, the United States, and Argentina, in order to have elements that serve as a reference for design work.

Anthropometric measurements of the human hand are of significant importance since they will allow us to design the prototype of a handheld myoelectric prosthesis based on the anatomy and biomechanics of the human hand. Therefore, the average measurements for the right hand (palm and phalanges) of women between the ages of 16 and 30 years are considered. As shown in Table 3.1, the dimensions for the phalanges are proposed, where the proximal phalanx was recorded between the metacarpophalangeal joint and the proximal interphalangeal joint; the medial phalanx, between the proximal and distal interphalangeal joints, and finally the distal phalanx between the distal interphalangeal joint and the end of the fingers, as shown in Figure 3.2. While Table 3.2 and Figure 3.3 show the length and width of the hand and the length of the palm[85].

Moreover, each finger joint has an active range of motion (ROM) which is the movement of the joint from its center. ROM can vary according to sex, age, daily activities, physical structure, etc. Table 3.3 describes the standard ROM on female finger joints, including flexion (blending) and extension (straightening) movements. So the Metacarpophalangeal joint (MCP) is when fingers meet hand bones, the Proximal interphalangeal joint (PIP) is the middle knuckle of the finger, and the Distal interphalangeal joint (DIP) is a knuckle below the fingernails. It is important to note that the thumb only has two phalanges: proximal and distal; as a result, all hand movements can be accomplished when the thumb is flexed at 90°.

Table 3.1: Lengths average of the phalanges of a woman's right hand's five fingers, expressed in cm, according to DIN 33.402 Standard. Adapted from Melo et.al. 2009[85].

Indicator	Description	Dimension (cm)
22	Width of the little finger in the palm	1,7
23	Width of the little near the yolk	1,5
24	Width of the ring finger in the palm	1,8
25	Width of the ring finger near the tip	1,6
26	Width of the middle finger in the palm	2
27	Width of the middle finger next to the tip	1,7
28	Width of the index finger in the palm	2
29	Width of the index finger next to the tip	1,7
30	Little finger length	6,6
31	Ring finger length	8
32	Middle finger length	8,5
33	Index finger length	7,6
34	Thumb length	6,9
35	Palm length	10,8

Figure 3.2: Measurements average of women's right-hand phalanges according to DIN 33.402 Standard. Adapted from Melo et.al. 2009[85].

Table 3.2: Length, width of the hand, and length of the palm of the woman's right hand, expressed in cm, according to DIN 33 402 Standard. Adapted from Melo et.al. 2009[85].

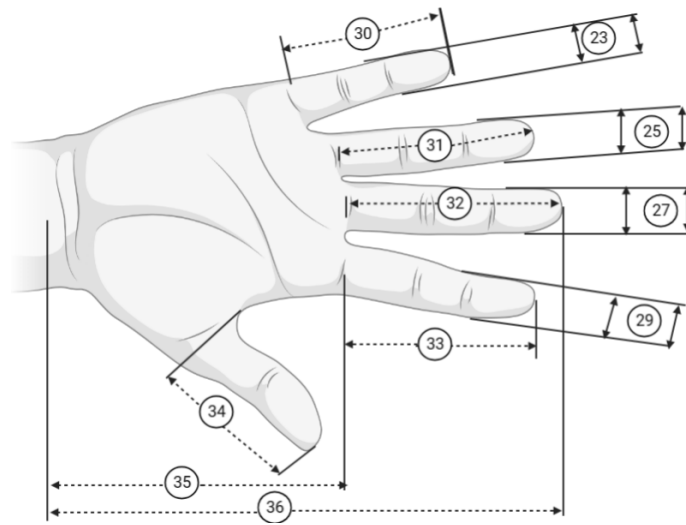| Indicator	Description	Dimension (cm)
36	Total hand length	19
37	Thumb width	2,1
38	Hand thickness	3,1
39	Width of the hand, including the thumb	10,1
40	Width of the hand, excluding the thumb	8,5
41	Hand grip diameter	15,7
42	The perimeter of the hand	20,7
43	The perimeter of the wrist joint	17,7
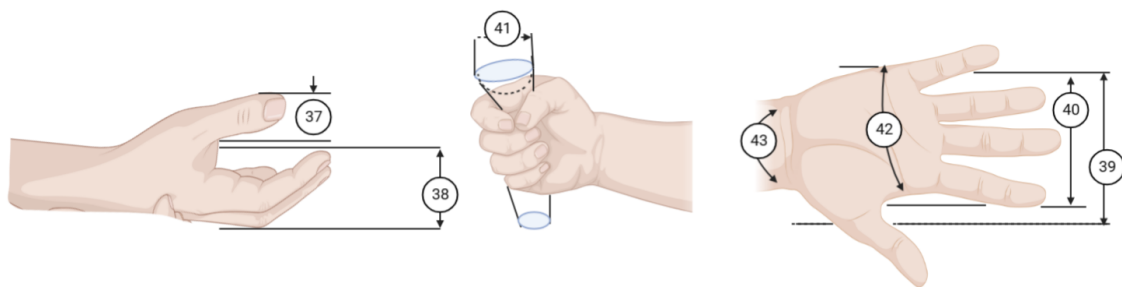
Figure 3.3: Measurements average of the right hand of a woman according to DIN 33.402 Standard. Adapted from Melo et.al. 2009[85].

Table 3.3: The range of motion (ROM) (°) for finger joints of the hand. Adapted from Wahit et.al. 2023[11] and Quinn et.al. 2023[86].

Finger joint	Motion range of fingers(°)	
	Thumb	Index, Middle, Ring, Little
MCP	60	[30 - 80]
PIP	-	120
DIP	90	80

3.2 Concurrent engineering (CE)

The methodology to be used for the design of the prototype of a myoelectric hand prosthesis is carried out through the criterion of Concurrent Engineering (CE), which allows establishing parameters prior to or before a design in order to generate solutions based on user suggestions in conjunction with the engineering bases and knowledge acquired for the development of the product[87]. The design proposed in this Project is intended to bring the product to market to be available to the patient. Furthermore, the product will function properly throughout its life cycle[88].

The proposed design comprises different stages. In order to make a decision based on the proposed design, it is necessary to evaluate each alternative after presenting it. The evaluation presented below refers to the alternative solutions established in the conceptual phase. This design seeks to create a prototype of a myoelectric hand prosthesis that fits the requirements and needs of patients. It aims to return much of the hand's functionality to the patient.

Among the solution principles generated during the conceptual design, the alternatives for the materialization design of the myoelectric hand prosthesis prototype are detailed below:

- Solution A: Titanium is an ideal material for printing myoelectric hand prostheses.

- Solution B: Printing technology for the myoelectric hand prosthesis with Acrylonitrile Butadiene Styrene (ABS) thermoplastic filament.

- Solution C: Aluminium is used to design and fabricate myoelectric hand prostheses.

- Solution D: Silicone is used to manufacture a myoelectric hand prosthesis.

As a result, the following endpoints were most decisive:

1. ***Ergonomics***, allows the patient to adapt to the prosthesis and not require too much force for performing a gripping movement.

2. ***Durability***, giving better mechanical resistance to the myoelectric hand prosthesis

3. ***Aesthetics***, show a natural appearance to the prosthesis and are customizable for the user.

4. ***Cost***, varies according to the manufacture type used for printing the myoelectric hand prosthesis.

From these initial data, is proceed through the following steps:

1. Evaluation of the specific weight of each criterion, as shown in Table 3.4.

Table 3.4: The specific weight of each criterion.

ergonomics >durability >aesthetic = cost						

Criterion	*Ergonomics*	*Durability*	*Aesthetic*	*Cost*	$\sum$ +1	*weighs*
Ergonomics		1	1	1	4	0.4
Durability	0		1	1	3	0.3
Aesthetic	0	0		0.5	1.5	0.15
Cost	0	0	0.5		1.5	0.15
				Sum	10	1

2. Evaluation of the specific weight of the ergonomics criterion, as shown in Table 3.5

Table 3.5: The specific weight of the ergonomics criterion.

solucion B >solucion A = solucion C >solucion D						

Ergonomics	*Titanium*	*ABS*	*Aluminium*	*Silicone*	$\sum$ +1	*weighs*
Titanium		0	0.5	1	2.5	0.25
ABS	1		1	1	4	0.4
Aluminium	0.5	0		1	2.5	0.25
Silicone	0	0	0		1	0.1
				Sum	10	1

3. Evaluation of the specific weight of the durability criterion, as shown in Table 3.6

Table 3.6: The specific weight of the durability criterion.

solution C = solution D >solution A >solution B						

Durability	*Titanium*	*ABS*	*Aluminium*	*Silicone*	$\sum$ +1	*weighs*
Titanium		0.5	0	0	1.5	0.15
ABS	0.5		0	0	1.5	0.15
Aluminium	1	1		0.5	3.5	0.35
Silicone	1	1	0.5		3.5	0.35
				Sum	10	1

4. Evaluation of the specific weight of the aesthetic criterion, as shown in Table 3.7.

Table 3.7: The specific weight of the aesthetic criterion.

solucion B >solucion C = solucion A = solucion B					

Aesthetic	*Titanium*	*ABS*	*Aluminium*	*Silicone*	$\sum$ +1	*weighs*
Titanium		0	0	0.5	1.5	0.15
ABS	1		1	1	4	0.4
Aluminium	1	0		1	3	0.3
Silicone	0 .5	0	0		1.5	0.15
				Sum	10	1

5. Evaluation of the specific weight of the cost criterion, as shown in Table 3.8.

Table 3.8: The specific weight of the cost criterion.

solucion B = solucion A >solucion C = solucion D					

Cost	*Titanium*	*ABS*	*Aluminium*	*Silicone*	$\sum$ +1	*weighs*
Titanium		0.5	1	1	3.5	0.35
ABS	0.5		1	1	3.5	0.35
Aluminium	0	0		0.5	1.5	0.15
Silicone	0	0	0.5		1.5	0.15
				Sum	10	1

Finally, a calculation of conclusions is shown in Table 3.9.

6. Table of conclusions:

Table 3.9: Calculation of conclusion.

Conclusion	*Ergonomics*	*Durability*	*Aesthetic*	*Cost*	$\sum$	*Priority*
Titanium	0,25 · 0,40	0,15 · 0,30	0,15 · 0,15	0,35 · 0,15	0,22	4
ABS	0,40 · 0,40	0,15 · 0,30	0,40 · 0,15	0,35 · 0,15	0,32	1
Aluminium	0,25 · 0,40	0,35 · 0,30	0,30 · 0,15	0,15 · 0,15	0,27	3
Silicone	0,10 · 0,40	0,35 · 0,30	0,15 · 0,15	0,15 · 0,15	0,19	2

Acrylonitrile Butadiene Styrene (ABS) is the best located, a short distance from Silicone material, followed by Aluminium material and Titanium material, which are far away. As a result, the myoelectric hand prosthesis was constructed using 3D printing technology with ABS thermoplastic filament because ABS is an ideal material for fabricating the hand structural parts of a prosthesis that meets ergonomic requirements, durability, aesthetics, and low cost.

3.3 Structural Design for myoelectric prosthetic hand prototype

In this section, the prototype of the myoelectric hand prosthesis was designed and assembled using CAD software because it has a sophisticated tool to facilitate rapid prototyping. Through the SolidWorks software 2022, each piece of the hand is designed, and it consists of four parts: (1) the palm, (2) the five phalanges, (3) the forearm socket that allows the connection between the residual limb and the prosthetic hand, and finally, (4) the electronic circuit.

First, the basic two-dimensional (2D) structure is drawn, where the structural elements are detailed in dimensions and proportions on the female hand. So, the dimensions of each piece for the prototype are established according to the anthropometric measurements of the anatomical structure of a woman's hand described in Table 3.1 and Table 3.2. A reference will also be made to Figure 4 because the prototype intends to mimic the human hand's structure. Following a three-dimensional (3D) model, it is possible to create the palm, five phalanges, a forearm socket, and electronic components. Afterward, the final assembly of a 3D model was tested, the respective modifications were made, and the prosthesis was simulated with three different types of grasping.

3.3.1 Palm Design

The design of the palm was made with average measurements of the length and width of the woman's right hand, detailed in Table 3.2 . Given the piece's dimensions to be designed, a two-dimensional (2D) design was sketched in SolidWorks, where the palm measurements were established. As a result, a three-dimensional (3D) structure is produced through the extrusion of the piece.

As indicated in Figure 3.4 in (a), the palm is rounded at the top, where the metacarpophalangeal joints (MCP) of the four fingers (index, middle, ring, and little finger) are inserted, but the thumb is in opposition to those fingers instead. In addition, in the inner part of the prototype of the palm (Figure 3.4 in (b)), the compartments where the servomotors will be located are observed to allow the movement of each phalanx to achieve a better aesthetic design for the person who uses this prosthesis, allowing the hand to move more freely and the objects to be gripped more securely.
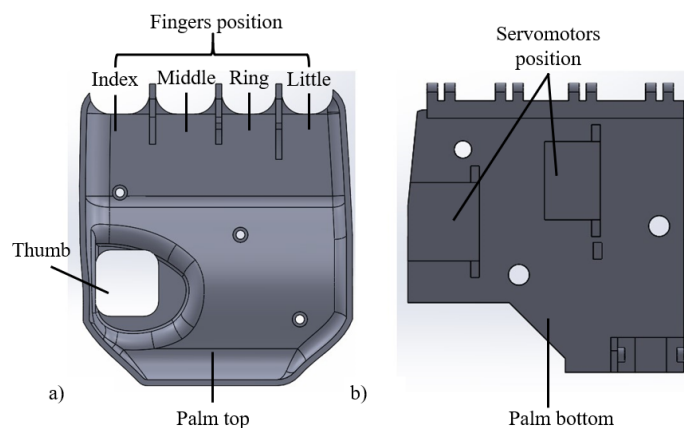

Figure 3.4: 3D Palm design: (a) palm top and (b) palm bottom.

3.3.2   Phalanx Design

The fingers of the human hand consist of three phalanges that are proximal, middle, and distal for four fingers (Index, Middle, Ring, and Little), unlike the thumb, which only consists of two phalanges (distal, proximal) and one metacarpal bone allowing the thumb to make the flexion and abduction movement inward from the palm. Table 3.1 shows the average phalange values of each finger of the woman's right hand used in designing the myoelectric hand prosthesis.

Based on this data, the pieces are made in SolidWorks, where a two-dimensional (2D) scaffold was drawn and then extruded to obtain a three-dimensional (3D) figure of each phalanx, as shown in Figure 3.5. Furthermore, round contours are applied to each phalanx, and it adapts to the metacarpophalangeal joint (MCP), proximal interphalangeal joint (PIP), and distal interphalangeal joint (DIP) joints, respectively, so that this structural design resembles the anatomy and biomechanist of the human hand. Therefore, the total number of joints in this myoelectric hand prosthesis was 14.
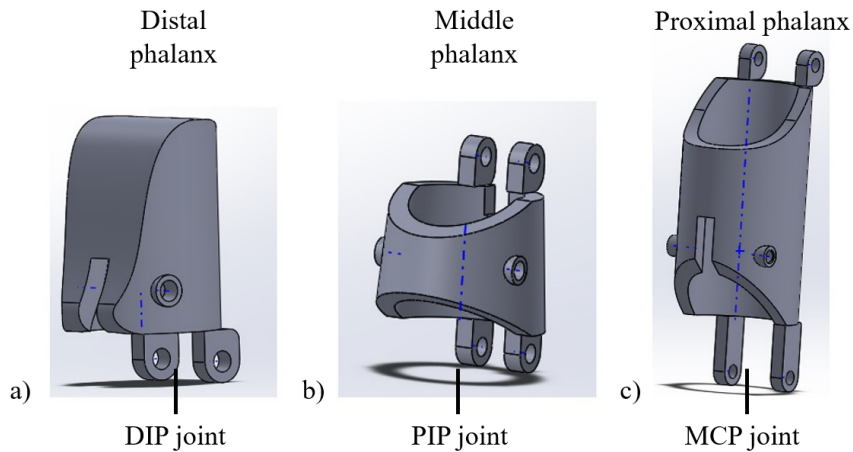
Figure 3.5: Design of phalanges for each finger: (a) the distal phalanx, (b) the middle phalanx, and (c) the proximal phalanx.

The phalanges connect each finger through the joints. For that, a solid connector creates, which is called a planar three-bar linkage mechanism for connecting to the servo motor and the myoelectric hand prosthesis that helps to move the joint and perform the grasping tasks, as shown in Figure 3.6 in (a). A three-bar linkage is connected in series because it represents the finger joints: MCP, PIP, and DIP. As a result, the phalanxes motion depends on each finger joint that allows rotation at a limited range of motion (ROM) of angles mentioned in Table 3.3 . Additionally, two mechanical stoppers are designed to protect the finger structure from being damaged when a servo motor applies an excess load on the myoelectric hand prosthesis. Figure 3.6 in (b) shows a 3D index finger model with a planar three-bar linkage structure; as mentioned above, it helps enhance the phalanges natural movement.
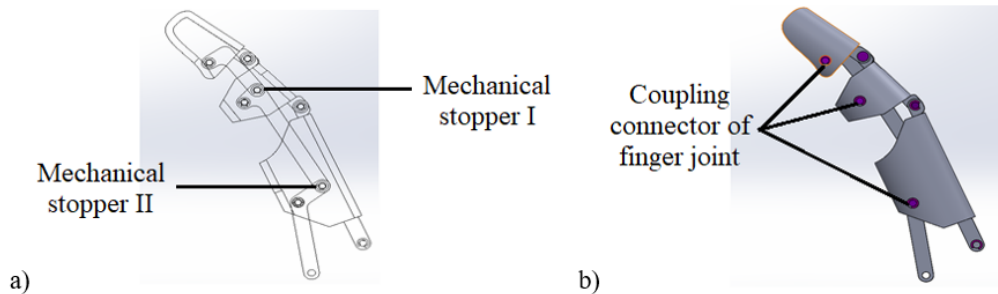
Figure 3.6: Index finger design: (a) planar three-bar linkage mechanism, (b) CAD model.

3.4 Defining the desired movements

The present design of the myoelectric hand prosthesis is a lightweight, integrated control system connecting EMG sensors directly to the hand. It gives the user an aesthetical and comfortable design to perform some functions of the natural hand in which all fingers work cooperatively. It can reproduce grips associated with stability and security, such as precision open grip, cylindric grip, and tip grip, following described each one of them.

3.4.1 Precision open grip

Small objects can be manipulated with the thumb in opposition with a precision open grip. When applying a close signal, the thumb moves to the midpoint range and pauses. The thumb finger is then active while the index, middle, ring, and little fingers remain extended, as shown in Figure 3.7.
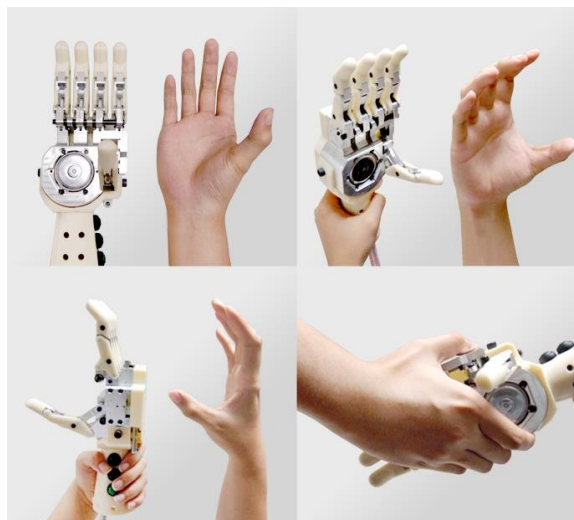
Figure 3.7: Precision open grip.

3.4.2 Cylindric Grip

The cylindric grip allows for easy and secure holding of round objects such as bottles, handles, and other household objects. The thumb finger is in opposition respect to the other fingers. Instead, the index, middle, ring, and little fingers are contracted until the object is taken and held secure, as shown in Figure 3.8.

Figure 3.8: Cylindric Grip.

3.4.3 Tip Grip

The tip grip brings the thumb in contact with the index finger, allowing the grasp of everyday items like pens, car keys, coins, and other small objects. The middle, ring, and little fingers close until they meet resistance or the close signal stop, as shown in Figure 3.9.

Figure 3.9: Tip Grip.

3.5 3D Model Assembly

A three-dimensional (3D) design of a prototype of a myoelectric hand prosthesis proposed for women that consider the human hand biomechanics described in sections 2.1 and 2.2 and the concurrent design requirements obtained in section 3.2. As a result, the myoelectric hand prosthesis was designed using 3D printing technology with Acrylonitrile Butadiene Styrene. (ABS) thermoplastic material because it presents a good mechanical performance besides the low cost for the manufacturing process of prosthesis, as shown in Table 4.4.

This prototype weighs 404 grams and has 2 degrees of freedom (DOF). The main components are the palm, five distal phalanges, four middle phalanges, five proximal phalanges, forearm socket positioned as

a missing limb, charger module, LIPO battery, micro servo motor SG90, wires, and circuit cover as shown in Figure 3.10 and Table 3.10. Each part of the design has been meticulously crafted to facilitate seamless interaction with electronic components. These components play a vital role in enabling the finger's opening and closing movements, as well as facilitating various grasping actions. The precision open movement allows for delicate and precise handling of objects, ensuring optimal control and accuracy. The cylindrical movement allows for a firm and secure grip, ensuring objects can be held securely in place. Finally, the tip movement ensures that even the most minute objects can be grasped with ease, offering versatility and adaptability in handling a wide range of items. With these electronic components seamlessly integrated into the design, the finger can perform intricate movements, enabling users to accomplish various tasks with dexterity and precision.
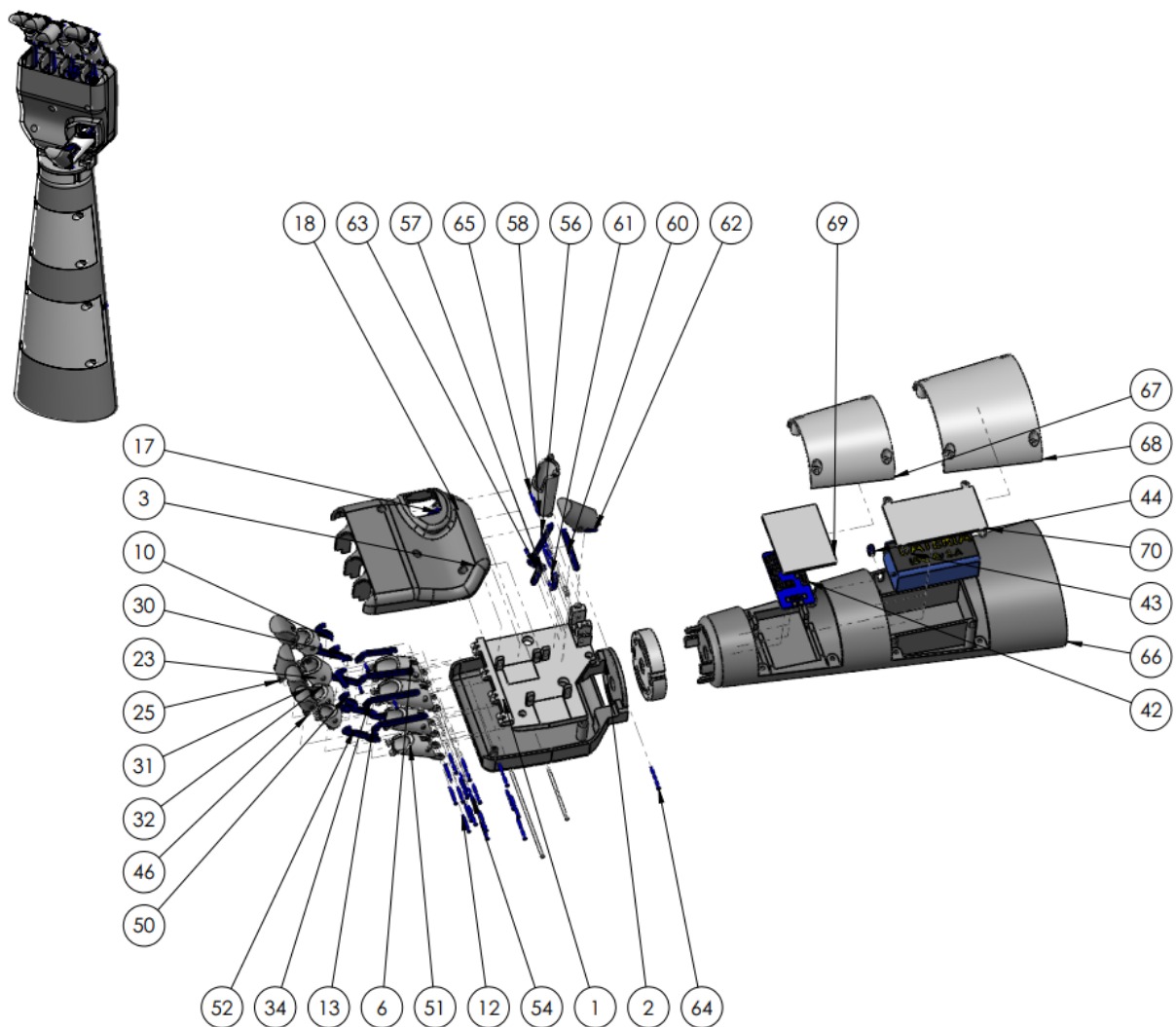

Figure 3.10: Design of the myoelectric hand prosthesis using CAD software.

Table 3.10: Components of the myoelectric hand prosthesis.

N. of element	Name of Piece	N. of element	Name of Piece
1	Palm	33	Proximal Phalanx round - Ring Finger
4	Wrist Attachment	34	Proximal Phalanx - Ring Finger
5	Medial Phalanx	42	Charger Module
6	Proximal Phalanx round	43	LIPO Battery
7	Distal Phalanx round	44	Battery Charging Pin
8	Index Finger - Proximal Phalanx	46	Distal Phalanx round - Little Finger
9	Index Finger - Medial Phalanx	49	Proximal Phalanx - Little Finger
10	Index Finger - Distal Phalanx	50	Distal Phalanx - Little Finger
18	SG90 - Micro servo motor 9g	51	Proximal Phalanx round - Little Finger
20	Distal Phalanx - Middle Finger	52	Middle Phalanx - Little Finger
21	Proximal Phalanx round - Middle Finger	53	Middle Phalanx round - Little Finger
22	Proximal Phalanx -Middle Finger	57	Servo motor Link
23	Medial Phalanx - Middle Finger	58	Proximal Phalanx - Thumb Finger
24	Proximal Phalanx - Middle Finger	59	Distal Phalanx - Thumb Finger
25	Distal Phalanx round - Middle Finger	66	Forearm
30	Distal Phalanx - Ring Finger	69	Circuit cover
31	Distal Phalanx round - Ring Finger	70	Battery cover
32	Medial Phalanx - Ring Finger		

3.6 Actuation

A servo motor was selected according to the torque and space of the myoelectric hand prosthesis design is a micro servo SG90. Chapter 4 contains more details about the calculations of how to select a correct servo motor for prothesis. Moreover, technical specifications are described in section 2.4. As indicated, it is tiny but offers an output torque of 1.8 kg.cm and holds objects of 0.44 kg approx. with a distance of 4 cm. Also, it achieves a 30 N pinch force. Micro servo motors SG90 is compatible with Arduino, and it is connected in parallel to the microcontroller allowing a rotation of 180 degrees (90 in each direction). The present Project uses three units of the micro servo motors SG90 to operate the thumb and index finger independently. The end servo motor operates dependently in a group of three (middle, ring, and little fingers).

3.7 Control System

The electronic system required to move the prototype of the myoelectric hand prosthesis consists of the control system and the actuation (servo motors). ATmega 328P is a microcontroller that was selected for controlling the prototype because is compatible with the library for the filtering of EMG signal. The dimensions of Arduino Uno are 68.6 mm x 53.4 mm, with a weight of 25 grams [89]. Externally battery is connected to the Arduino Uno, but an analog input requires a 5V of power supply, for that is necessary to make a conversion because a battery works in a range of 7-12V. Figure 3.11 shows a scheme of the voltage conversion performed as necessary because if the power supply voltage range exceeds, the MCU gets damaged.
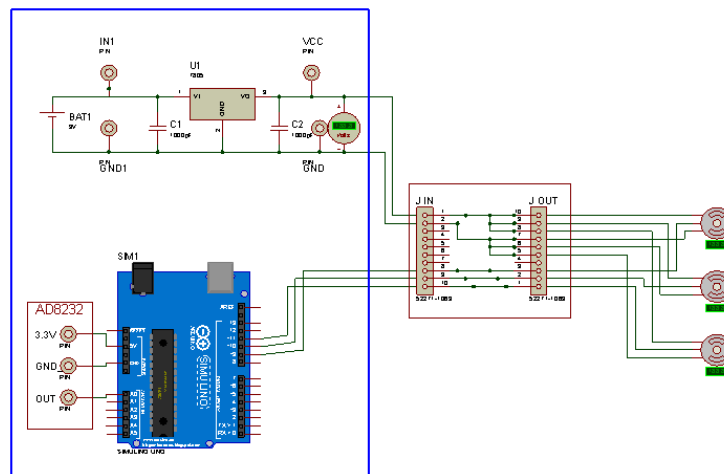
Figure 3.11: Schematic design for voltage conversion using Proteus software.

3.8 Power source

The system's power supply is connected to the microcontroller and micro servo motors SG90. The maximum current draw of a micro servo motor SG90 under a stall condition is 360mA, but when being commanded to move from 100mA to 250mA. A rechargeable Lithium-ion polymer (LiPo) battery of 7.4 V and 3000 mAh capacity is selected for the prosthesis. Li-Po battery weighs 120 grams and is located inside the forearm socket of the myoelectric hand prostheses.

3.9 EMG measurement

The present Project used gel electrodes that work on the principle of chemical equilibrium, detecting the change between the muscle surface and body skin through electrolytic conduction; also, it is non-invasive

for the user. When a surface electrode detects a signal, an EMG signal is processed with an AD8232 module which is an integrated signal. Biopotential signals can be challenging to detect due to large amounts of noise created by motion sensors or remote electrode placements; for this reason, it is designed to extract, amplify and filter small signals[90],[91]. This design allows an embedded microcontroller to acquire the output signal easily. Then, data from AD8232 module is transmitted using the Arduino Uno microcontroller, which connects the USB port of the microcontroller to the personal computer (PC) for obtaining a digital signal that observes in the LabVIEW 2022 software interface.

3.10 EMG analysis

Surface electromyographic (EMG) signal is measured with conventional gel electrodes to detect the muscular contraction when the user performs hand gestures such as precision open grip, cylindrical grip, and tripod grip. EMG signals record a biopotential difference between the two detecting and the reference electrodes used to control the prosthesis. For acquiring the EMG data, two electrodes are positioned on the skin region at Flexor Digitorum Superficialis (FDS) and Extensor Digitorum Communis (EDC)[29],[92]. Whereas a reference electrode is placed where no electric potential is expected, as shown in Figure 3.12.
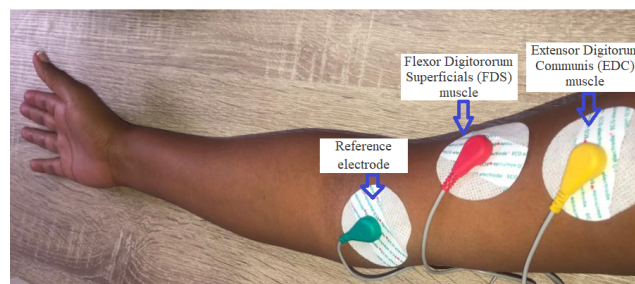
Figure 3.12: Electrodes placement over muscles to detect the muscular activity.

3.10.1 Signal Acquisition and Processing

Electromyography signal acquisition system consists of four main stages: (1) signal collection, (2) signal amplification, (3) signal filtering, and (4) analog to-digital converting. Considering that a muscle contractions are small in amplitude range from 0 μV to 10 mV, and since other biosignals may be present around the muscle, electrode placement is essential to achieve an adequate signal-to-noise ratio (SNR). The filtering stage impacts the quality of EMG signals. In order to optimize the quality of the received signal, it should be denoised, rectified, and filtered. As the AD8232 module has an operational amplifier to allow designing a high-pass a low-pass filter. Then, the data is fed into an Analogue to Digital Converter. (ADC) . As part of the design of the ADC stage, three main variables must be taken into account: the open-loop gain used during the amplification stage, the maximum output voltage at the system's back-end for acquiring EMG signals, as well as additive noise[56]. Additionally, a sampling frequency for the ADC stage is determine, obtaining a digital signal that is observed in the LabVIEW 2022 software interface. Figure 3.13 shows a diagram of EMG signal acquisition and processing.
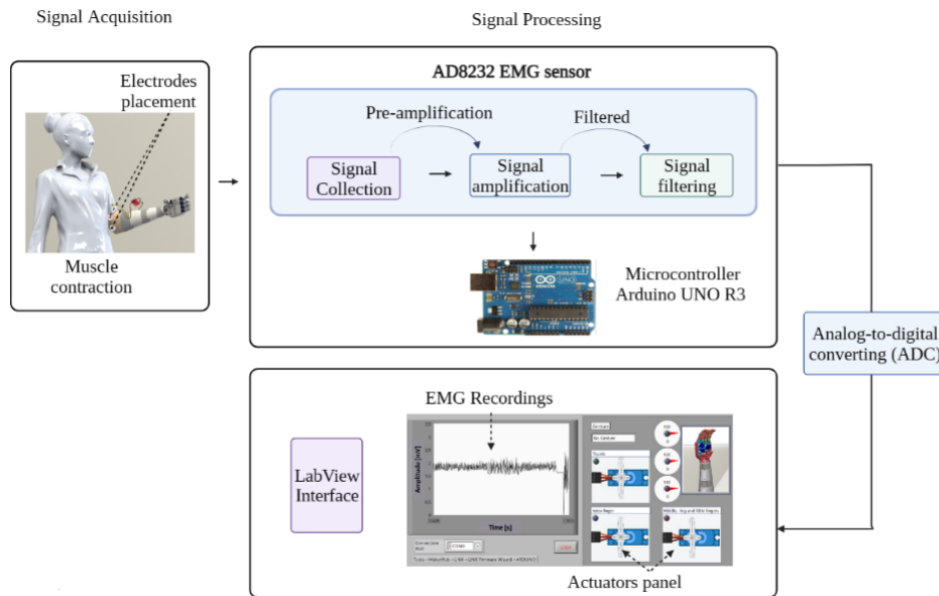
Figure 3.13: Block diagram of EMG signal acquisition and processing in LabVIEW software interface.

3.11 Structural Analysis

A structural simulation of the myoelectric hand prosthesis is performed using Simsolid software. In the simulation, a workload of 1 kg is applied, and a gravity force of 9.8 is placed on the structure (phalanges); as a result, the mass distribution will be according to gravity. The bottle is rigid and does not deform; this condition was applied so that it is transmitted to the fingers since it is the place of support where the load goes.

The experimental setup for the static analysis of cylindric grip is represented in Figure 3.14. In (a) is shown the 3D model with its Force direction and the gravitational force as well as the fixed constraint. In (b) an illustration from the lateral view of the myoelectric prosthetic hand while grasping a cylindrical object is presented.
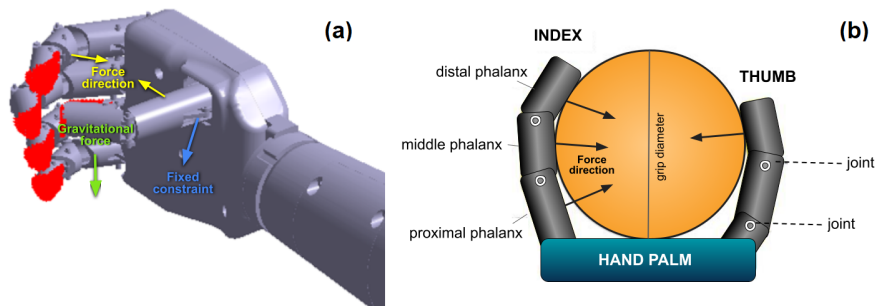
Figure 3.14: Experimental setup of the static analysis for cylindric grip.

Chapter 4

Results

The results analysis of the main characteristics of myoelectric hand prosthesis prototype start with the design requirements where the design of the prototype, weight, costs and pinch force are included. Then, for an appropriate analysis and in order to identify possible shortcomings of the material, as well as information or the prototype flows a simulation is presented which supports interpretation of the most important variables to system performance. Grasping Tasks are simulated and analyzed through their maximum displacement and Von misses stress. Finally, EMG signal measurement, processing and analysis results are exposed.

4.1   Design requirements

4.1.1   Prototype design

The design of the prototype was based on the anatomy of the human hand. The dimensions, proportions, and functionality of a real human hand served as the basis for every component of the prosthetic hand. The concept of the suggested prosthesis was based on mimicking human finger motions. Real human hand phalanges were 3D scanned for the prosthetic phalanges design, which was then created using CAD (computer-aided design) or computer-based software to aid in design processes. In this study specifically SolidWorks software 2022 was applied, the same 3D drawing program was used to model the entire prosthetic hand structure, including the actuators and processing supports.

All hard elements were constructed by using 3D printing technology with ABS filament that has good functional and structural characteristics and that are suitable for future 3D printing. As mentioned in the previous section of Methodology, the prototype design consists of four parts: (1) the palm, (2) the five phalanges, (3) the forearm socket that allows the connection between the amputated limb (residual limb) and the prosthetic hand, and finally, (4) the electronic circuit.

According to the literature, the human hand consists of Carpal bones, Metacarpal bones, Proximal, Middle and Distal Phalanges. In this study, the prototype presents movement only for the fingers (three phalanges for little, ring, middle and index fingers, as well as only two phalanges for thumb). Further, for the Metacarpal and Carpal bones there is no movement because of they are included in the rigid palm design. Additionally, round contours are applied to each phalanx, and it adapts perfectly to the

metacarpophalangeal joint (MCP), proximal interphalangeal joint (PIP), and distal interphalangeal joint (DIP), respectively. So that this structural design resembles the anatomy and biomechanism of the human hand with a total of 14 joints, as can be seen in Figure 4.1. Also, for each finger CAD model with their respective kinematic scheme and detailed isometric views are presented in Annexes included in Chapter 7 (for thumb, index, middle, ring and little fingers, respectively).
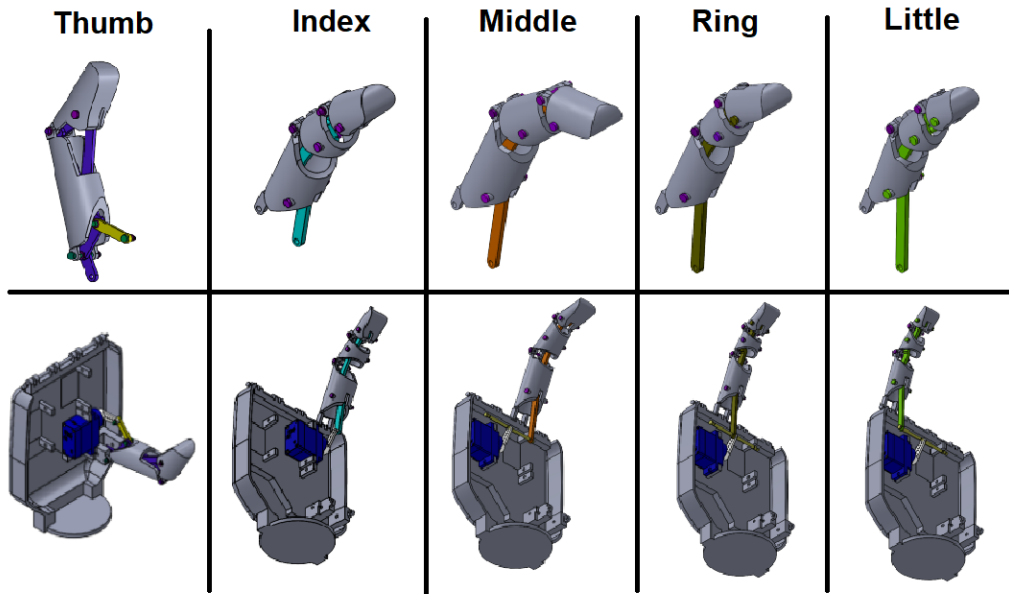
Figure 4.1: Isometric view for the fingers of myoelectric hand prosthesis prototype.

In terms of the 3D model assembly, the prototype weighs around 404 grams and has 2 Degrees of Freedom. (DoF) due to the extension and flexion movements with respect to the frontal plane. In Table 4.1 are expressed the final Joint flexion (MCP, PIP and DIP) angles reached by each finger of the prototype of myoelectric hand prosthesis. The main components, as seen in the Figure 3.10 (in Chapter 3 of Methodology), are the palm, five distal phalanges, four middle phalanges, five proximal phalanges, forearm socket positioned as a missing limb, charger module, Li-PO battery, micro servo motor SG90, wires, and circuit cover.

Table 4.1: Joint flexion (MCP, PIP and DIP) angles.

Finger	MCP Angle (°)	PIP Angle (°)	DIP Angle (°)
Thumb	8.8	-	49.4
Index	23.7	20.1	9.8
Middle	23.7	30.1	29.9
Ring	23.5	11.1	26.4
Little	19.8	20.4	12.6

4.1.2 Costs

Table 4.2 provides a summary of the prototype's material costs. The total of material costs were approximately 158.80 dollars. The 3D printing costs of the myoelectric Hand prosthesis are based on the use of 750 grams of ABS. Costs for labor and equipment are excluded from the cost calculation.

Table 4.2: Material costs of the myoelectric hand prototype.

Part	Costs in dollars
Filament for 3D printing	*48.00*
Micro servo motor SG90	*9.00*
ATMEGA 328P-PU microcontroller	*7.00*
Arduino Uno R3	*19.80*
AD8232 EMG Sensor Module Kit	*25.00*
Jumper wires	*4.00*
Lipo battery - 7.4V - 3000mAh	*46.00*
Total	**158.80**

4.1.3 Weight

The weight of the prototype of Myoelectric Hand prosthesis is about 404 grams. A summary of the material weighs of the myoelectric hand prototype components is presented in Table 4.3. The battery is included in this measurement, the weight of the Lipo battery used is about 120 g.

Table 4.3: Material weighs of the myoelectric hand prototype components.

Part	Weight (grams)
3D printed parts	*167*
Micro servo motor SG90	*27*
ATMEGA 328P-PU microcontroller	*10*
Arduino Uno R3	*25*
AD8232 EMG Sensor Module Kit	*5*
Jumper wires	*50*
Lipo battery - 7.4V - 3000mAh	*120*
Total	**404**

4.1.4 Pinch Force

The pinch force of the myoelectric hand prosthesis will be evaluated. The requirement was set at 30 N. So, the pinch force has been measured at three different servo motor SG90 speeds. The measured forces are shown that the pinch force for the thumb and index fingers is 17.65 N; instead, for the middle, ring, and little fingers is 5.88 N for each one. Figure 4.2 shows the micro servo motor SG90 rotates at 70 degrees at a time of 1.5 seconds; therefore:

$$70° \cdot \tfrac{\pi}{180°} = 1.221 rad$$
$$r = \tfrac{1.221 rad}{1.5 s}$$
$$r = 0.815 \tfrac{rad}{s}$$

Servomotor speed calculation
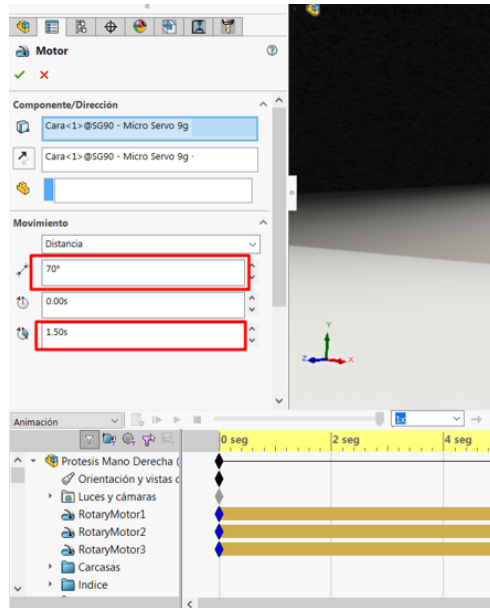
Figure 4.2: Micro servo motor SG90 speed.

The Micro Servomotor SG90 datasheet provides information about torque and distance. The following are described of them.

Parameters:

Torque : $T = 1.8 Kg \cdot cm = 0.1765\ N \cdot m$
Distance: D = 2 cm = 0.02 m
Pinch force: F = 30 N
Ratio : $r = 0.82 \tfrac{rad}{s}$

Where:

$$T = F \cdot d$$

$$F = \tfrac{T}{d} = \tfrac{0.1765 N \cdot m}{0.02 m}$$

$$F = 17.65\ N$$

This force is divided into three in the case of the middle, ring, and little fingers.

$$F = 5.88 \text{ N}$$

Moreover,

$$Weight = mass \cdot gravity$$
$$m = \tfrac{17.65}{9.81}$$
$$\text{m} = 1.79\text{kg}$$

The weight of a 1 liter bottle is equal to 1 kg. Therefore, the Myoelectric Hand Prosthesis supports the bottle's weight.

4.2   Structural design evaluation

For the desired movements defined previously in the Methodology the application of Finite element analysis is needed to predicting how the prototype will react to forces, and other real-world physical effects. In this regard, the final assembly of the complete 3D model was tested by simulation (applying Simsolid Software) for three different types of grasping which are detailed below.

4.2.1   Grasping Tasks Simulation

Basically, a grasping task can be defined as a series of joint movements with the goal to clasping the fingers on an object. In this study are analyzed and reproduced the precision open, cylindric and tip grips.

In precision open-hand gripping is when the fingers are stretched out and the middle knuckle straight. This is the least stressful grip position since the joints are straight. Open-hand grip is the kind of grip that allow to pick up large, awkward objects without convenient handles. In general, these objects are things that are big enough to prevent wrapping the thumb around fingers as in a traditional barbell lift or lifting something with a thin handle. In this study, the prototype of the myoelectric prosthesis is able to reproduce the precision open-hand grip as shown in (a) of Figure 4.3).

Cylindrical gripping, is one in which the thumb is positioned in opposition and the entire hand is in touch with the object. This grasp is often referred to as a gross grasp. Also, in this research project is presented the cylindrical grip as can be seen in (b) of Figure 4.3).

In tip grip, the most common form of precision grip, the pads of the thumb and index fingers are placed in opposition to one another to pick up or pinch a small object (such as a tiny bead, pencil, or grain of rice). In this study, the prototype of the myoelectric prosthesis is able to position the thumb and index finger so that a pencil is held (as shown in (c) in Figure 4.3).
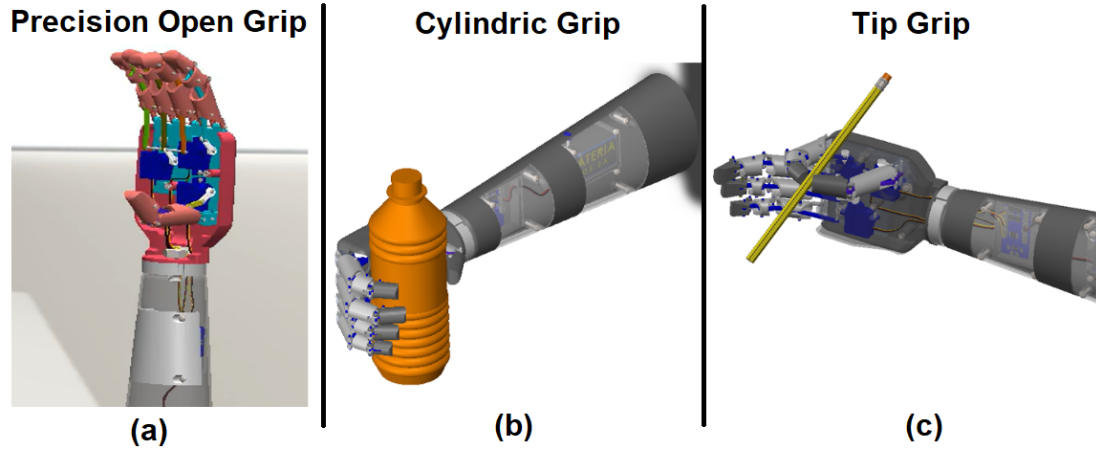
Figure 4.3: The myoelectric hand prosthesis postures for (a) Precision open grip, (b) Cylindric grip and (c) Tip grip.

4.2.2 Structural Analysis

As we know, every material has a specific yield strength depending on their properties. The mechanical properties, such as elastic modulus, mass density, ultimate tensile strength, compressive yield stress and thermal expansion coefficient of the ABS material applied for the prototype analysis are shown in Table 4.4.

To determine parameters on the functioning of the prosthesis and its structural integrity, different weighs have been applied for the cylindrical object grip system that is the most frequently used in activities of daily living and which allows to evaluate more accurately the force exerted by the prosthesis on a solid object since there are a greater number of contact points.

Table 4.4: Mechanical properties of ABS material developed with Simsolid software 2022.

Mechanical properties	Value	Units
Elastic Modulus	$2.78e-09$	Pa
Poisson's Ratio	$4.00e-01$	dimensionless
Mass Density	$3.57e-02$	kg/m^3
Ultimate Tensile Strength	$5.41e-07$	Pa
Compressive yield stress	$5.44e-07$	Pa
Thermal expansion coefficient	$6.70e-05$	$1/(°C)$

When finite elements perform the simulation, the software first calculates the displacements, which do not vary when the elements, loads, contour functions, and others are already well-defined. The stress distribution of the mechanism was identified through the analysis of the hand simulator. These calculations will show a variation because meshing works with triangles, tetrahedrons, and hexahedrons, so according to this, the nodes will appear the deformations. The structural analysis of CAD model using SimSolid

software is presented in Figure 4.4, where can be identified a cylindric grip with a greater stress distribution at the end of the fingers just in the distal phalanges (in red), specifically at the pads which are in contact with the object.

In addition, the software analyzes the connections of the isostatic system; in this case, the system's connections are rigid since they form a solid, so they work according to the von Mises stress mathematical criterion and Maximum displacement. It is important to be mindful of the fact that the part where the user enters the residual limb, the palm and wrist of the prototype is immobile (remains fixed) in this analysis.
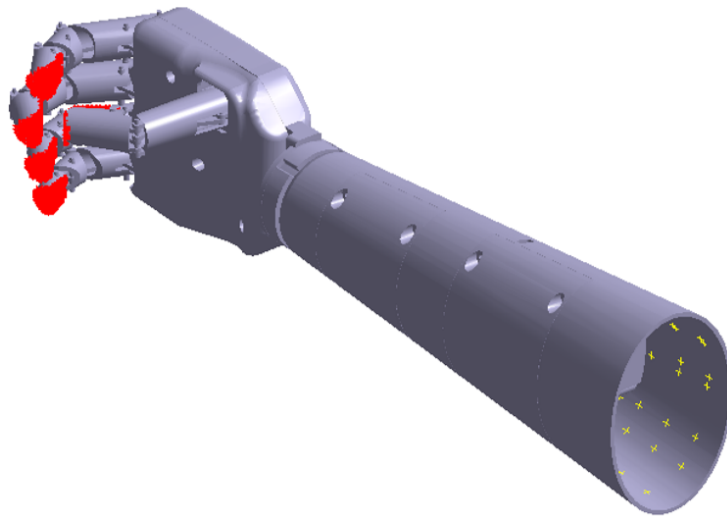
Figure 4.4: Structural analysis of CAD model using Simsolid software.

Von misses stress

Finite element model is implemented in SimSolid to analyze stress distributions in the proximal and distal components of prototype and to evaluate candidate sites for design optimization. Boundary conditions are set on distal, middle and proximal phalanges components: all simulate the respective rotations and the hard-stops in contact with their frames.

Linear analyses present a relevant increase in the von Mises stress values. For all simulations, when the weight of the object is increased the von Mises stress maximum value was mainly concentrated at the middle and distal phalanges (in red and orange) evidencing the greater points of contact and the sites where was exerted a major force over the cylindric object, in other words, where peak values (maximum) of Von Mises stresses are reached. As outputs of the numerical simulations described previously, Figure 4.5 shows the Von Mises stress for the myoelectric hand prosthesis at different applied Forces. In regards to force (a) 39,2 [N], (b) 58,8 [N], (c) 78,4 [N], (d) 98 [N], and (e) 117,6 [N] are applied, respectively.

Also, for each one are highlighted (in green) the critical finger regions, where deformations takes place. As can be seen, in five fingers the pads located at the distal phalanx area and the thin edge near the distal rotation axis are compromised as a result of the applied force.

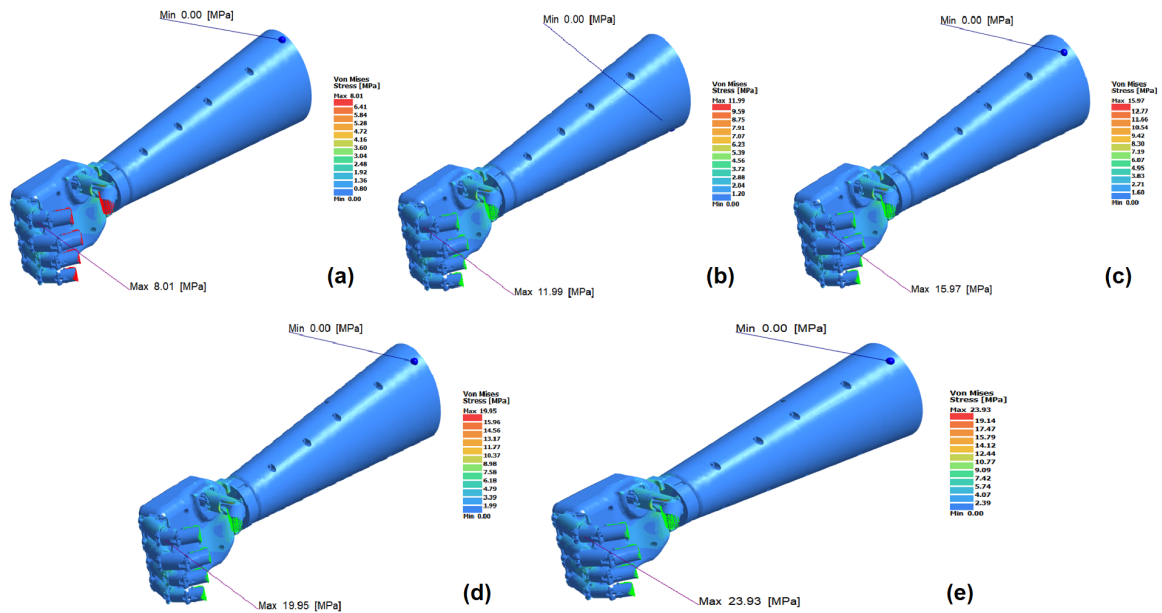Figure 4.5: Computational results in terms of Von Mises stresses (in MPa) for the myoelectric hand prosthesis prototype.

Maximum displacement

A complete analysis requires to know the maximum values for which the structure of the prototype remains intact or without experiencing some type of deformation. For this, values of the maximum displacement were obtained, which is the measure of how much the ABS used in this study for the design of the myoelectric prosthesis can be deformed before reaching its point of failure (breakdown point).

To evaluate this, five different forces were applied to the cylindrical grip. As outputs of the numerical simulations, Figure 4.6 shows the computational results in terms of maximum displacement evidencing that the increase in force is directly proportional to the increase in material deformation. The most compromised areas are the distal phalanges, especially in the internal area or the one corresponding to the finger's pads.

According to the plot of applied Force (measured in Newtons) in terms of displacement (measured in mm) Figure 4.7 shows that an approximately force of 120 N is reached the maximum displacement equivalent to 6 mm, or described in other words at this point the prototype starts to experience some type of deformation until break down. As a consequence, it can be said that the prototype only supports objects with weighs lower than 12 Kg. However, in order to maintain the integrity of the structural design is better to apply weights lower than 10 Kg to avoid the yield limits.

Below, a summary of the Maximum values of the structural analysis in terms of Von Mises stresses expressed in MPa units and Maximum displacement indicated in milimeters are shown in Table 4.5.
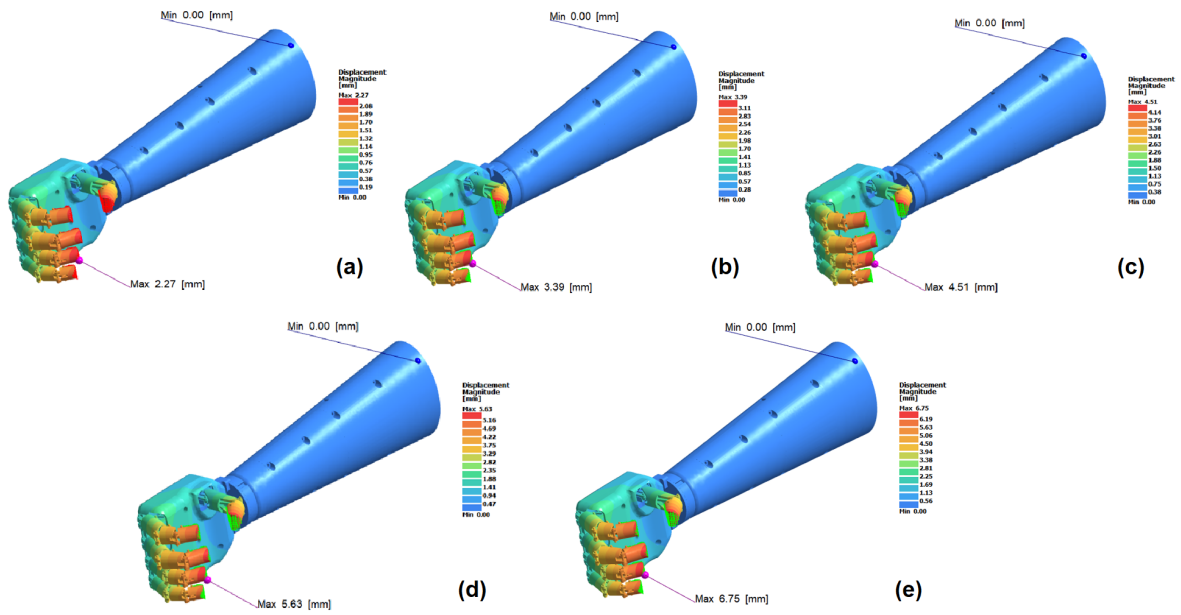
Figure 4.6: Computational results in terms of Maximum displacement (in mm) for the myoelectric hand prosthesis prototype.
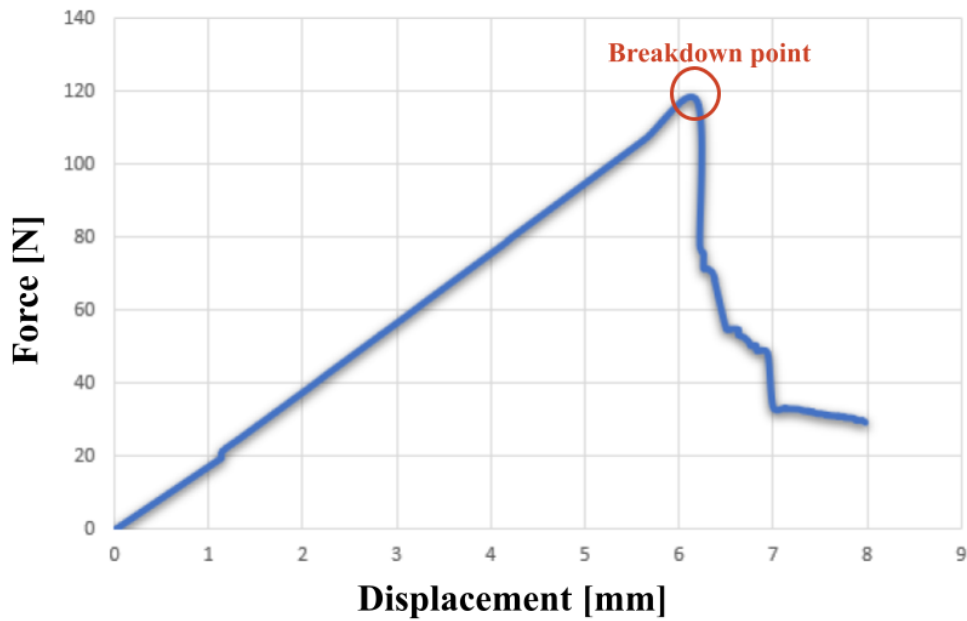
Figure 4.7: Output of applied Force [N] in terms of displacement [mm] for the myoelectric hand prosthesis prototype.

Furthermore, in Figure 4.8 is shown (in yellow) the palm and phalanx areas where greatest tensile strength is applied. In other words, is shown where the maximum stress that the prototype can bear before breaking or deforming when it is stretched or pulled. In this regard, the safety factor lies between the closed interval given by 1.2 and 9.4. The tensile yield stress is equal to 30 MPa and the Compressive yield stress is equivalent to 30 MPa.

Table 4.5: Maximum values of Structural Analysis.

Maximum values of Structural Analysis		
Force (N)	**Von Mises Stress (MPa)**	**Displacement Magnitude (mm)**
39.2	8.01	2.27
58.8	11.99	3.39
78.4	15.97	4.51
98.0	19.95	5.63
117.6	23.93	6.75
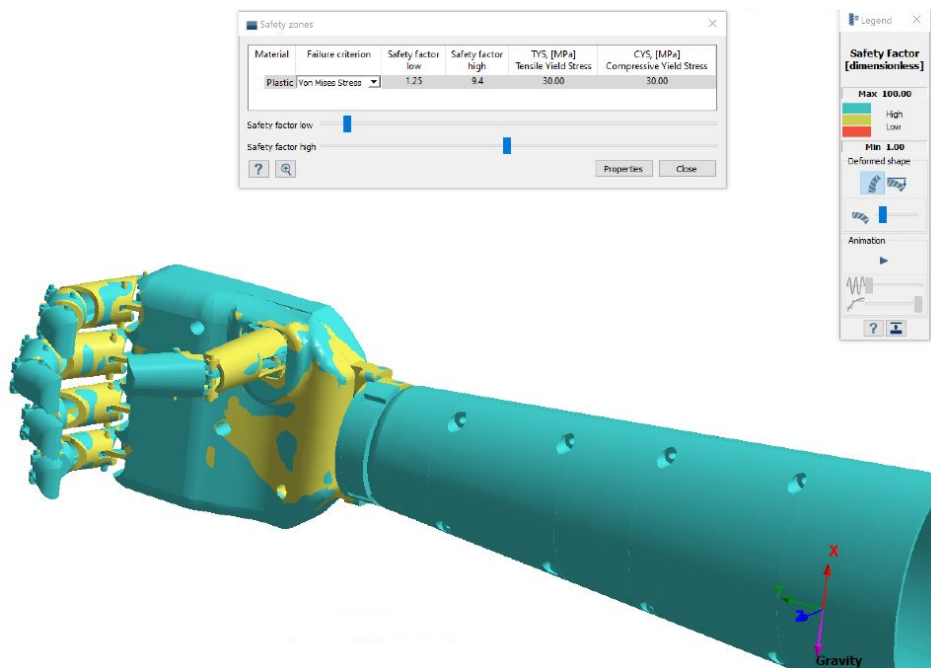
Figure 4.8: CAD software model with safety and unsafety zones for the prototype.

4.3 EMG signal acquisition

Placing solid gel electrodes over the arm muscle is a control system for myoelectric hand prosthesis proposed as shown in Figure 4.9 where it could obtain signals corresponding to movements for the grasping objects. In order to demonstrate the functioning of the myoelectric system, surface EMG signals are studied by simulating hand movement from healthy women. Data collection has an equivalent to 16 seconds with a sampling frequency (Fs) of 1 KHz and follows the next steps: the first 3 seconds, an 'precision open' is recognized. After, the fingers apply force for 6 seconds when the fingers take a water bottle; this movement is called cylindric grasping. Continue with 3 seconds of precision open, and finally, the last 4 seconds correspond to a tip grip.
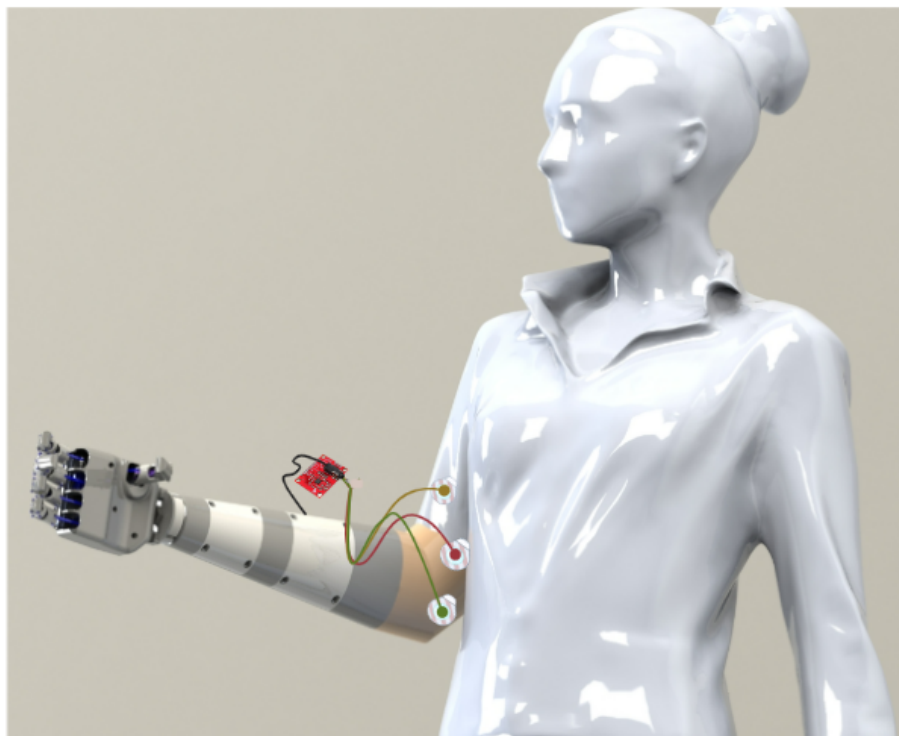
Figure 4.9: Control System for myoelectric hand prosthesis.

4.3.1 Gesture recognition using surface EMG sensor

The myoelectric hand prosthesis described in Chapter 3 presents a design that resembles the human hand's biomechanics to allow hand movements for grasping different objects, such as precision open grip, cylindric grip, and tip grip. Therefore, the EMG signal levels are determined by muscle activity intensity which was recorded and stored on a personal computer to be processed using LabVIEW software 2022. The reader can see the signals obtained by following the procedure mentioned above. The spectrogram shows the time-varying spectral representation of the EMG signal. The spectrogram represents the time data on the x-axis, the frequency representation on the y-axis, and the amplitude of the frequency-time pair is

color-coded.

A physical signal is received from the EMG sensor AD8232 module and has to be sent to LabVIEW via Arduino ATmega328P. An EMG waveform was recorded when the user performed three hand movements for grasping objects, as shown in Figure 4.10. Duration of each reading was 3 seconds for a precision open grip, 6 seconds for a cylindric grip, and 4 seconds corresponding for a tip grip. All the data were acquired at a sampling rate 1 KHz. Additionally, a specific gain value is determined at which their signal-to-noise ratio is maximum because as an EMG systems gain is increased beyond a specific value, baseline noise increases, which decreases its SNR.

As can be seen in Figure 4.10, in all EMG signals when the user does not require any force the signal is constant over the time. However a minimal or significant variation in amplitude translates in a change in the force produced by the muscle. For the cylindric grip in Figure 4.10 in (b), it is evident a significant increase of amplitude due to the major points of contact and the force required for the user when all the fingers are closed to take a bottle of water. For the tip grip as shown in Figure 4.10 in (c), the minimal force exerted on the thumb and index fingers is evidenced with the increase in amplitude over the time . And finally, for the precision open grip is observed in Figure 4.10 in (a) a very little variation as a result of the reduced movement.
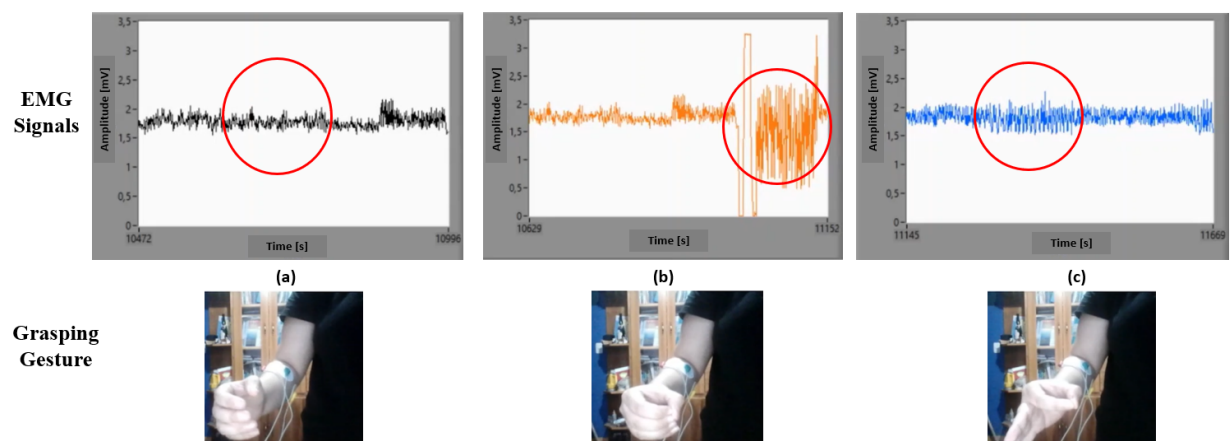

Figure 4.10: The frequency spectrum of EMG signal obtained from a gesture recognition for: (a) precision open grip, (b) cylindric grip, and (c) tip grip.

Chapter 5

Discussion

5.1 Evaluation of the design requirements

The development of a useful, affordable prototype of myoelectric hand prosthesis was the main objective of this study. In order to fulfill this goal different variables that are relevant for its correct functioning are discussed and evaluated. A number of design requirements have been satisfied in the prototype design. Among the fundamental features in this study the 3D printing material, actuation, control system, as well as the measurement and analysis of EMG bio-signals are discussed. In addition, in the two last sections the prototype is compared in terms of other alternatives of CAD software and the obtained signals from other research studies.

5.1.1 Material Prosthetic hand

There are several opinions on the use of 3D printing in the field of prosthetics, especially the viability of this type of technology in the manufacture of biomedical devices above all of prostheses is questioned. According to Setty et.al, 3D printing applied to the manufacture of prosthetics is a growing practice with great potential due to its versatility[93]. Two years later, Setty stated that this innovative technique is viable due to the quality of the printed products, however he refers to the improvements in terms of printing speed to be used in prosthetics. Setty also mentioned that laser sintering in orthopedic printing maintains a high standard and is also recommended for printing prosthetic products, as it is much faster[94].

In general, 3D printing has opened the door to a number of possibilities. With the rise of 3D printing, several innovative technologies have also been developed that require different materials depending on the application you want to give it. There are materials that vary in their properties, at present, according to the bibliographic review there are filaments made from synthetic, natural components as well as the combination of both or with extraordinary luminiscent, magnetic and conductive properties. The industry has more than 26 filaments, among them are: PLA, ABS, PETG, TPE, TPU, TPC, Nylon (PA), Polycarbonate (PC), Wood-filled, Metal-filled, Environmentally-friendly, Conductive and Luminiscent, Magnetic, Color changing, Dichromatic, Clay/Ceramic, Carbon fiber, Glass fiber, Metal, high impact polystyrene (HIPS), PVA, Wax/Castable, ASA, Polypropylene, PC-ABS, Polyoxymethylene and PMMA[95].

According to Chonga, S. et.al, the three of the most commonly used 3D printing filaments are Polylactic Acid. (PLA), nylon and ABS by their low cost and extensive availability[96]. These materials can be extruded into basic desktop 3D printers and they are accessible because a coil is about $20. Regarding

nylon, it is a flexible plastic that provides a new set of characteristics to the filaments. Nylon is tougher and more chemically resistant than PLA and ABS, but it also has less resistance[95]. In this case, not meeting the minimum strength requirements, the nylon of the following comparison is omitted since it is not compatible with the objective of this hand prototype.

Both, PLA and ABS are thermoplastics. Contrary to metals, which experience plastic deformation after their yield stresses, PLA and ABS are recognized for their compound elastic and plastic behavior after reaching the material's yield stress[97]. PLA is consider a suitable material because this as an eco-friendly and biodegradable alternative. In terms of printing it has good adhesion at high speeds and its convenient due to its ability to produce sharp corners. In general, PLA is less prone to warping. However, during the printing process is required a fan at the extruder and in general it can be fairly brittle and susceptible to heat which become it not ideal for long-term outdoor use and with a limited gluing feature.

On the other hand, ABS is one of the most resistant materials to high-temperature environments like sunlight or hot water. It presents good adhesion at high printing speeds, it is slightly flexible and requires smooth extrusion. ABS is recognized by their easy sanding and gluing. Among the disadvantages of 3D printing using ABS filament are the chemical odors that can be given off during extrusion. In addition, when undergoing heating and cooling stages, it can present variations in its dimensions since it can expand or shrink, so a heated plate is required for printing. For prosthetic purposes, ABS is weaker and less rigid, but also stronger and lighter, making it a more suitable plastic for prototyping applications.

According to Alkhatib et.al, mechanical properties derived from the tested 3D printed PLA and ABS samples shows a greater mass density for PLA ($1.30 g/cm^3$) compared with ABS ($1.10 g/cm^3$). In addition, regarding the stiffness of the material measured by Young's modulus, it is evidenced that PLA with a value equal to 3.90 GPa is more rigid or in other words, is less prone to deformations compared to ABS which has a value equal to 1.40 GPa. Also, in terms of the maximum load that these materials can support without fracture when being stretched, PLA presents a value of 54.00 MPa in comparison with ABS which is around 32.00 MPa[98]. In terms of costs, both PLA and ABS are similar for each kilogram of filament (1.75 mm). In this research study, is applied ABS for 3D printing because the prototype requires a material capable of withstanding loads without neglecting its ability to be flexible. But above all, it is much lighter providing greater comfort to the patient.

5.1.2   Actuation

Prosthetic hands are enhancing its efficiency and utility in terms of force grip and precision to grasp objects based on an appropriate number points of contact. Mata Amritanandamayi et.al, mentioned that an upper limb prosthetic are essentially based on pneumatic and hydraulic actuators, as well as electrically driven by a motor[99]. Among the available electrical-actuators they can be separated in three categories: DC motors, stepper motors and servo motors.

According to the literature, feedback is used by servo motors to regulate their position, speed, or torque so they are less prone to error. Besides, without the requirement for input, a stepper motor can be directed to a specified position, but overload could cause it to lose synchronism[100]. For these before mentioned limitations, stepper motor is discarded for prosthetic purposes due to all type of devices used for medical purposes require to maintain total control over the variables. In addition, micro DC motors are also discarded because of their high initial cost, and additionally by their maintenance costs due to the presence of the commutator and brushes. The brushes' short lifespan as a result of friction wear is a significant drawback[84].

For this study, electrical actuation has compatible properties for the prototype because it is widely commercially available, relatively easy to implement and low cost[101]. Among the options, this study implemented servo motors (three servo motors SG90) due to their compatibility with the control system, capability to provide the required force, besides they represents a cost effective, easy implementation and widely available alternative.

As mentioned before, one of the most important requirements for properly actuation is a pinch force equivalent to 30 N. In this study, three servo motors are used obtaining a pinch force of 52.95 N. For the middle, ring and little fingers a pinch force equal to 5.88 N is reached for each one. While, for index and thumb individually a total pinch force of 17.65 N is obtained.

5.1.3 Control system

The actuator activation and the EMG signal analysis require a control system, so Microcontrollers. (MCU's) are used for that purpose. An electronic circuit containing a central processing unit (CPU) and memory is known as a microcontroller. It is a synchronous digital circuit that contains both firmware code (the program memory) and data generated during the code execution (the data memory)[102].

Awad et.al mentioned that the Arduino Atmega is an open-source microcontroller that is based on the ATmega328P. It can be programmed in C++, Python, or another programming language. Also, it has 14 digital input and output pins, 6 analog inputs, a 16 MHz quartz crystal oscillator, a USB port connection, a power jack, an ICSP header, and a reset button. Moreover, it runs at a voltage of 5V and is used as a USB-to-serial to converter for a serial comunication, allowing to connect a computer through a USB port[103],[104]. Unlike an Arduino, a Raspberry Pi is a small and hackable MCUs. It has built-in USB Graphics and wireless Bluetooth, allowing programming codes that runs within a Linux, Windows, or Mac OS operating system; as a result, it is more complex to operate. It has input pin and output pins to control other electronic components[105],[106].

Despite many types of microcontrollers on the market ranging in features and complexities, the Raspberry Pi is relatively large compared to the Arduino MCU's. This project used Arduino UNO because it offers an open-source platform and can be programmed using widely computational software like Matlab, LabVIEW, Simulink, and others. Also, the price of Arduino UNO R3 is 19.80, and weighs 25 g. During simulation, a gel electrode was used for EMG signal detection; therefore, a Raspberry Pi would be overkilled; consequently, an Arduino would be a better choice for that.

5.1.4 EMG measurement

Electromyography. (EMG) is a biomedical signal obtained from the electrical stimulus of the nerves generated in the CNS. In addition to providing information about neuromuscular diseases, EMG signals can be used to diagnose injuries to any body muscle. When EMG signals are monitored, it is possible to identify myocardial and muscle failures as well as characterize a user's intention of movement[55]. Physiological control signals acquired by sensors can be used to determine the user's intent for controlling the hand prosthesis. Therefore, an electrodes measure the level of activity by recording the electrical activity within them. According to Gohel et.al [51] a multiple types of electrodes to detect the EMG signal are available on the market. Two main types of electrodes can be distinguished: an invasive and non-invasive electrodes.

According to the literature, a needle electrode is an invasive electrode inserted inside the muscle or implanted to measure EMG [107]. Because needle electrodes require surgery skills for implant through the skin, these are complex, expensive, and have safety risks from the user's [108]. Meanwhile, a wet electrodes of Ag/AgCl (silver chloride) needs a conductive gel to ensure good electrical contact, the gel is applied between the electrode and the skin in a period of time until complete diffusion of the gel over the layers of skin. These electrodes provide some disadvantages, such as gel deterioration, causing poor long-term performance of measurement; in addition, the electrode is rigid, which prevents it from adhering correctly to the skin; it can also cause skin irritations and allergies [109]. Thus, Rayo et.al [109] indicates that an alternative is the employment of dry electrodes (metal electrodes) because the skin does not require a previous preparation with gel.

On the other hand, gel electrodes allow muscular activity detection and are easy to apply over muscle. This commercial electrode consists of three electrodes and an AD8232 module, which is an integrated and works as an operational amplifier that helps to easily obtain a clear signal [110]. As a result, gel electrodes were used because they detect biopotential signals such as electromyography (EMG) or electrocardiogram (ECG). In addition, gel electrodes can find at a low cost of 25 dollars; this allows us to reduce the manufacturing costs of myoelectric hand prosthesis to make them accessible.

5.1.5   Power source

The power source for actuation can varies according the design choice of the actuation type. Luchetti et. al [111] estimated that an average prosthesis hand is used 360 times a day, which corresponds to a median of 130.000 times per year. In order to, the myoelectric hand prosthesis will be need a high power capacity to control system (MCU's), actuator, and other components. The lithium-ion polymer (LiPo) battery is a lightweight, long-lasting, and powerful solid-state battery that provides a constant supply of energy. Instead of a nickel metal hydride battery (NiMH) is an energy storage system that depends on charge/discharge reactions. NiMh has high power capacity, is safe, provides good tolerance, and is compatible [112]. Both lithium-ion polymer (LiPo) and NiMH are a rechargeable batteries [113],[114].

Since electric actuation is selected, a rechargeable Lithium polymer (LiPo) battery of 7.4 V and 3000 mAh capacity is selected for the power the entire system of prosthesis. Although these batteries can swell or otherwise explode over time, checking the user guide for proper use is always recommended [112]. In this way, it offers the user greater security when using a prosthesis.

5.2   CAD software Comparison

Analyzing the contact interactions between prosthetic fingers and diverse objects has proven to be successful with the use of finite element analysis [115]. Mushtaq et.al [116] mentioned that in engineering, a 3D design is used due to the ease of creating prototypes and components using computer-aided design (CAD). So, technology intends to make engineering processes more efficient with tools for conceptual design, product layout, strength, dynamics analysis, and more. The following Table 5.1 shows a comparison of CAD software for 3D design. (1) Solidworks, (2) Autodesk Inventor, and (3) Fusion 360.

As a result, SolidWorks was used in this Project as it differs from other software for the following reasons. As mentioned Tran et.al [117] SolidWorks generates three files relating to 3D basic concepts: parts, assembly, and drawings. In order to allow to create, simulate, publish, and manage 3D models.

Table 5.1: Comparison of a 3D CAD software for design.

3D CAD Software			
Criteria	*Solidworks[117]*	*Inventor[118]*	*Fusion 360[119]*
User Interface	Simple	Simple	A powerful software
Capabilities	An industry leader	A professional-grade	More power full
Parts Library	Component library management	Component library management	N/A
Rendering	It is better in many ways	It requires plugging to help	It is pretty close
Electronic	An electrical wiring library	Design for manufacturability	Design electronic components, but they do not have actual properties
Simulation	Dynamic simulation	Cloud simulation and simplify	Required Cloud Coins

Additionally, it has high simulation capabilities to help users test products and performance against real-life circumstances with an analytical property. Also, Software help to identify and resolve complicated assembly issues during the early stages of product development. Finally, it does have a larger user community and so when you go want to look for learning resources it is much easier to find those for Solidworks.

On the other hand, Autodesk Inventor is like SolidWorks because it deals with separate files for parts assemblies, bodies, and components created and dealt with as one entity, designing, visualizing, and simulating products before they are built [118]. Instead, Fusion 360 is a cloud-based 3D software [119] that is like designing parts from the assembly levels, depending on needs where it is possible to animate and render the designs.

5.3 Software for EMG signals acquisition

There are several factors that affect EMG signals of upper extremities, including the user's physiological changes, external noise, electrode position, and so on. As a result, researchers are developing algorithms to improve the control of prosthetic devices by improving the accuracy of EMG signals. The following table 5.2 describes the main features of some software used in the acquisition of EMG signals.

Table 5.2: Features of some software used in the acquisition and processing EMG signals.

Method	Algorithms	Features	Ref.
EMG Feature extraction	*Artificial Neutral Networks (ANN)*	- Adjust the coefficient of multiplication vectors for each epoc. - It is made up of three or more interconnected layers.	[71], [120]
	Linear Discriminant Analysis (LDA)	- Its good classification accuracy and computational efficiency. - It separates two or more classes because is a supervised dimensionality reduction technique. - It achieves competitive accuracy of 97.4%	[120]
	K-Nearest Neighbor (KNN)	- It is based on traditional machine learning techniques. - It considering the similarity of the dataset samples in the training set.	[121], [70]

5.4   Limitations

This project was created effectively, achieving the intended objectives; however, limits were discovered during the development of the design of prototype of myoelectric hand prosthesis, such as acquiring the EMG signals from a single user due to time restrictions. Nevertheless, the intended prototype was created using the physiological signal obtained. Additionally, this study offers a wide range of possibilities for future development, from transferring the analog signal acquisition prototype to a board to avoid noise to optimizing the prototype using microelectronics and nanoelectronics.

Modern technology allows EMG signals to be acquired and processed more efficiently signals can now be acquired and processed more efficiently. In this project, gel electrodes were used, which are inexpensive and accessible. Despite this, since the electrodes are disposable, the user must learn the position to place them to achieve the signal required for the different types of grip proposed. The detection of the signal can be improved by using another type of EMG sensor, such as the MYO armband (by Thalmic Labs), or by developing an algorithm that allows the signals to be classified into different channels, resulting in high levels of EMG signal precision when combined with artificial intelligence.

Chapter 6

Conclusions and Outlook

6.1   Conclusions

In general, prosthetic devices require several parameters to enhance manufacturing of high-performance. The absence of evidence supporting the use of inexpensive myoelectric prostheses served as the motivation for this study. This undergraduate research project proposed and developed a functional and low-cost 3D design of a myoelectric hand prosthesis for women, which works similarly to the human hand. It aims to adapt to tasks related to Activities of Daily Life. (ADL) as well as the ergonomic and aesthetic demands of each patient.

To summarize, anthropometric measurements of the prototype report a length of 19 cm, a thickness equivalent to 3.1 cm, and a width equal to 10.1 cm, in agreement with DIN 33.402 standard. In order to generate solutions with the engineering bases, the criterion of Concurrent Engineering. (CE) was applied, demonstrating that 3D printing technology with ABS thermoplastic filament is suitable for this purpose. More in detail, the prototype design consists of four parts (1) the rigid palm (including the Metacarpal and Carpal bones), (2) the five fingers (two phalanges for the thumb, three phalanges for the little ring, middle, and index fingers), (3) the forearm socket that allows the connection between the residual limb and the prosthetic hand, and finally, (4) the electronic circuit.

The final 3D model assembly weighs around 404 grams and has 2 DoF due to the extension and flexion movements concerning the frontal plane. The structural design resembles the anatomy and biomechanism of the human hand with a total of 14 joints which allows to simulate the motion of precision open, cylindrical, and tip grips. The electronic system required to move the prototype of the myoelectric hand consists of an Arduino UNO R3 for the control system and three micro servo motors SG90 to operate the thumb and index fingers independently and in a group of three for the other ones as the actuation setup. A rechargeable Lithium-ion Polymer (LiPo) battery of 7.4 V with a 3000 mAh of capacity is selected for the power source.

The prototype was optimized through a myoelectric signal acquisition by the AD8232 EMG sensor module kit. It was implemented for more natural control and more time-efficient. In order to demonstrate the functioning of the myoelectric system, surface EMG signals are studied by simulating hand movement from healthy women using LabVIEW software. Data collection has an equivalent of 16 seconds with a sampling frequency of 1 KHz.

Besides, one of the most essential requirements for properly actuation is a pinch force equivalent to 30 N. In this study, a total pinch force of 52.95 N is obtained. For the middle, ring, and little fingers, a pinch force equal to 5.88 N is reached for each one. While for the index and thumb individually, a total pinch force of 17.65 N is obtained. In order to predict how the prototype will react to forces and distribution of stress and to ensure a valuable and stable prototype, together with the identification of possible shortcomings, a simulation is performed. The precision open, cylindric, and tip grips are reproduced in this study. For finite elements analysis, different weighs have been applied for the cylindrical object grip with a diameter of 15,7 cm because it is the most used in activities of daily living. It was analyzed through their stress distribution indicated by maximum displacement, and Von misses stress.

According to the mechanical properties of ABS and prosthesis structure, simulation reports a direct relationship between weight (i.e Force) and maximum displacement. A force of 120 N is reached the maximum displacement equivalent to 6 mm, or described in other words, at this point, the prototype starts to experience some type of deformation until it breaks down. In this regard, the outputs of the numerical simulations can determine that the distal phalanx area and the thin edge near the distal rotation axis are compromised due to the applied force.

Also, for all simulations, when the weight of the object is increased, the von Mises stress maximum value was mainly concentrated at the middle and distal phalanges evidencing the greater points of contact and the sites where was exerted a major force over the cylindric object, in other words, where peak values (maximum) of Von Mises stresses are reached. As a consequence, it can be said that the prototype only supports objects with weights lower than 12 Kg. However, to maintain the integrity of the structural design is better to apply weights lower than 10 Kg to avoid the yield limits.

6.2   Future Works

A Convolutional Neural Networks (CNN) can be implemented for the processing and classification of EMG signals in order to carry out the myoelectric control of the prosthesis. In addition, other types of EMG sensors can be used, such as the Myo armband that facilitates the placement of the device on the user's arm or develops an electrode-based bracelet to reduce the manufacturing cost of the prosthesis and make it accessible. On the other hand, for the design of a myoelectric hand prosthesis, the current model moves five fingers while the wrist is fixed. However, the wrist can be designed to offer full rotation to allow different movements to be executed in the prosthesis, and the user will be able to grasp objects with a greater force and perform complex tasks to generate more DoF and offers better functionality to the prosthesis.

Bibliography

[1] Goislard De Monsabert, B.; Edwards, D.; Shah, D.; Kedgley, A. Importance of consistent datasets in musculoskeletal modelling: a study of the hand and wrist. *Annals of Biomedical Engineering* **2018**, *46*, 71–85.

[2] Melo, J.; Villacis, N.; Segura, C.; Segura, L.; Loza, D. Study of art and construction of 1 GDL hand prosthesis for partial amputation of hand. *Science Robotics* **2017**, 23.

[3] Schlesinger, G. *Der Mechanische Aufbau der Kunstlichen Glieder. Ersatzglieder und Arbeitshilfen, part II*; Springer Berlin, 1919.

[4] Smit, G. Mechanical evaluation of the "Hüfner hand" prosthesis. *Prosthetics and Orthotics International* **2020**, *45*, 61.

[5] Reiter, R. Eine neue elektrokunsthand. *Grenzgebiete der Medizin* **1948**, *1*, 133–135.

[6] Zuo, K. J.; Olson, J. L. The evolution of functional hand replacement: From iron prostheses to hand transplantation. *Plastic Surgery* **2014**, *22*, 44–51.

[7] Biddiss, E. A.; Chau, T. T. Upper limb prosthesis use and abandonment: a survey of the last 25 years. *Prosthetics and orthotics international* **2007**, *31*, 236–257.

[8] Belter, J. T.; Segil, J. L.; SM, B. Mechanical design and performance specifications of anthropomorphic prosthetic hands: a review. *Journal of rehabilitation research and development* **2013**, *50*, 599.

[9] Biddiss, E.; Beaton, D.; Chau, T. Consumer design priorities for upper limb prosthetics. *Disability and rehabilitation: Assistive technology* **2007**, *2*, 346–357.

[10] Bastarrechea, A.; Estrada, Q.; Zubrzycki, J.; Torres-Argüelles, V.; Reynoso, E.; Rodríguez-Mendez, A.; Coutiño, E. Mechanical design of a low-cost ABS hand prosthesis using the finite element method. **2021**, *1736*, 012039.

[11] Wahit, M. A. A.; Ahmad, S. A.; Marhaban, M. H.; Wada, C.; Izhar, L. I. 3d printed robot hand structure using four-bar linkage mechanism for prosthetic application. *Sensors (Basel, Switzerland)* **2020**, *20*.

[12] Calado, A.; Soares, F.; Matos, D. A review on commercially available anthropomorphic myoelectric prosthetic hands, pattern-recognition-based microcontrollers and sEMG sensors used for prosthetic control. **2019**, 1–6.

[13] Marino, M.; Pattni, S.; Greenberg, M.; Miller, A.; Hocker, E.; Ritter, S.; Mehta, K. Access to prosthetic devices in developing countries: Pathways and challenges. **2015**, 45–51.

[14] Shaw, R. P. *Social health insurance for developing nations*; World Bank Publications, 2007.

[15] Cuellar, J. S.; Smit, G.; Breedveld, P.; Zadpoor, A. A.; Plettenburg, D. Functional evaluation of a non-assembly 3D-printed hand prosthesis. *Proceedings of the Institution of Mechanical Engineers, Part H: Journal of Engineering in Medicine* **2019**, *233*, 1122–1131.

[16] CONADIS, Consejo Nacional para la Igualdad de Discapacidades. 2021; `https://www.consejodiscapacidades.gob.ec/estadisticas-de-discapacidad/`.

[17] Manero, A.; Smith, P.; Sparkman, J.; Dombrowski, M.; Courbin, D.; Kester, A.; Womack, I.; Chi, A. Implementation of 3D printing technology in the field of prosthetics: past, present, and future. *International journal of environmental research and public health* **2019**, *16*, 1641.

[18] Ruiz-Olaya, A. F.; Burgos, C. A. Q.; Londoño, L. T. A Low-Cost Arm Robotic Platform based on Myoelectric Control for Rehabilitation Engineering. **2019**, 0929–0933.

[19] Drake, R. L.; Gray, H.; Vogl, W.; Mitchell, A. W. *Gray's anatomy for students*; Elsevier Health Sciences TW, 2015.

[20] He, Z.; Wakabayashi, A.; Yurievich, R. R.; Sekiguchi, M.; Kang, Y.; Shin, D. Development of a Prosthetic Hand Based on Human Anatomy. *International Journal of Electronics and Electrical Engineering* **2019**, *7*, 17–20.

[21] Xu, Z.; Todorov, E. Design of a highly biomimetic anthropomorphic robotic hand towards artificial limb regeneration. **2016**, 3485–3492.

[22] Hurtado-Manzanera, P. A.; Luviano-Cruz, D.; Vidal-Portilla, L. Design and construction of a prototype of myoelectric prosthesis. Mundo Fesc. **2018**, *15*, 14–25.

[23] Feix, T.; Romero, J.; Schmiedmayer, H.-B.; Dollar, A. M.; Kragic, D. The grasp taxonomy of human grasp types. *IEEE Transactions on human-machine systems* **2015**, *46*, 66–77.

[24] Panchal-Kildare, S.; Malone, K. Skeletal anatomy of the hand. *Hand clinics* **2013**, *29*, 459–471.

[25] Kumar, A.; Mundra, T. S.; Kumar, A. Anatomy of Hand. *Encyclopedia of Biometrics* **2014**, 28–35.

[26] Tang, A.; Varacallo, M. *StatPearls - Anatomy, shoulder and upper limb, hand carpal bones*; StatPearls Publishing, 2021.

[27] Maw, J.; Wong, K. Y.; Gillespie, P. Hand anatomy. *British Journal of Hospital Medicine* **2016**, *77*, C34–C40.

[28] Cuellar, J. S.; Plettenburg, D.; Zadpoor, A. A.; Breedveld, P.; Smit, G. Design of a 3D-printed hand prosthesis featuring articulated bio-inspired fingers. *Proceedings of the Institution of Mechanical Engineers, Part H: Journal of Engineering in Medicine* **2021**, *235*, 336–345.

[29] Abdallah, I. B.; Bouteraa, Y.; Rekik, C. Design and development of 3D printed myoelectric robotic exoskeleton for hand rehabilitation. *International journal on smart sensing and intelligent systems* **2017**, *10*, 1–26.

[30] Bullock, I. M.; Borràs, J.; Dollar, A. M. Assessing assumptions in kinematic hand models: a review. **2012**, 139–146.

[31] Komatsu, I.; Lubahn, J. D. Anatomy and biomechanics of the thumb carpometacarpal joint. *Operative Techniques in Orthopaedics* **2018**, *28*, 1–5.

[32] Norose, M.; Nimura, A.; Tsutsumi, M.; Fujita, K.; Okawa, A.; Akita, K. Anatomical study for elucidating the stabilization mechanism in the trapeziometacarpal joint. *Scientific Reports* **2022**, *12*, 20790.

[33] Fontaine, C.; D'agostino, P.; Maes-Clavier, C.; Boutan, M.; Sturbois-Nachef, N. Anatomy and biomechanics of healthy and arthritic trapeziometacarpal joints. *Hand Surgery and Rehabilitation* **2021**, *40*, S3–S14.

[34] Woo, S. H. *The Thumb: A Guide to Surgical Management*; Springer, 2019.

[35] You, W. S.; Lee, Y. H.; Oh, H. S.; Kang, G.; Choi, H. R. Design of a 3D-printable, robust anthropomorphic robot hand including intermetacarpal joints. *Intelligent Service Robotics* **2019**, *12*, 1–16.

[36] Tieland, M.; Trouwborst, I.; Clark, B. Skeletal muscle performance and ageing. J Cachexia Sarcopenia Muscle 9: 3–19. http s. *doi. org/10.1002/jcsm* **2018**, *1223*.

[37] Mirakhorlo, M.; Visser, J. M.; Goislard de Monsabert, B.; Van der Helm, F.; Maas, H.; Veeger, H. Anatomical parameters for musculoskeletal modeling of the hand and wrist. *International Biomechanics* **2016**, *3*, 40–49.

[38] Rapp, F. A.; Soos, M. P. *StatPearls - Anatomy, Shoulder and Upper Limb, Hand Cutaneous Innervation*; StatPearls Publishing, 2021.

[39] Soubeyrand, M.; Assabah, B.; Bégin, M.; Laemmel, E.; Dos Santos, A.; Crézé, M. Pronation and supination of the hand: Anatomy and biomechanics. *Hand Surgery and Rehabilitation* **2017**, *36*, 2–11.

[40] Mansfield, P. J.; Neumann, D. A. *Essentials of kinesiology for the physical therapist assistant e-book*; Elsevier Health Sciences, 2018.

[41] Liu, Y.; Zeng, B.; Jiang, L.; Liu, H.; Ming, D. Quantitative Investigation of Hand Grasp Functionality: Thumb Grasping Behavior Adapting to Different Object Shapes, Sizes, and Relative Positions. *Applied Bionics and Biomechanics* **2021**, *2021*.

[42] Stival, F.; Michieletto, S.; Cognolato, M.; Pagello, E.; Müller, H.; Atzori, M. A quantitative taxonomy of human hand grasps. *Journal of neuroengineering and rehabilitation* **2019**, *16*, 1–17.

[43] Parry, R.; Macias Soria, S.; Pradat-Diehl, P.; Marchand-Pauvert, V.; Jarrassé, N.; Roby-Brami, A. Effects of hand configuration on the grasping, holding, and placement of an instrumented object in patients with hemiparesis. *Frontiers in neurology* **2019**, *10*, 240.

[44] Perez, M. A.; Rothwell, J. C. Distinct influence of hand posture on cortical activity during human grasping. *Journal of Neuroscience* **2015**, *35*, 4882–4889.

[45] Institute for Quality and Efficiency in Health Care (IQWiG), How do hands work? - InformedHealth.org - NCBI Bookshelf. 2018; `https://www.ncbi.nlm.nih.gov/books/NBK279362/`.

[46] Duncan, S. F.; Saracevic, C. E.; Kakinoki, R. Biomechanics of the Hand. *Hand Clinics* **2013**, *29*, 483–492, Management of Hand Fractures.

[47] Lee, K.-S.; Jung, M.-C. Ergonomic evaluation of biomechanical hand function. *Safety and health at work* **2015**, *6*, 9–17.

[48] Pu, S.-W.; Chang, J.-Y.; Pei, Y.-C.; Kuo, C.-C.; Wang, M.-J. Anthropometry-based structural design of a hand exoskeleton for rehabilitation. 2016.

[49] Lapresa, M.; Zollo, L.; Cordella, F. A user-friendly automatic toolbox for hand kinematic analysis, clinical assessment and postural synergies extraction. *Frontiers in Bioengineering and Biotechnology* **2022**, *10*.

[50] Serbest, K.; Cilli, M.; Eldogan, O. A dynamic virtual hand model for estimating joint torques during the wrist and fingers movements. *Journal of Engineering Science and Technology* **2018**, *13*, 1665–1676.

[51] Mehendale, N.; Gohel, V. Review on Electromyography Signal Acquisition, Processing and Its Applications. *Gohel, V., Mehendale, N. Review on electromyography signal acquisition and processing. Biophys Rev (2020). https://doi. org/10.1007/s12551-020-00770-w* **2020**,

[52] Jamal, M. Z. In *Computational Intelligence in Electromyography Analysis*; Naik, G. R., Ed.; IntechOpen: Rijeka, 2012; Chapter 18.

[53] Yamanoi, Y.; Ogiri, Y.; Kato, R. EMG-based posture classification using a convolutional neural network for a myoelectric hand. *Biomedical Signal Processing and Control* **2020**, *55*, 101574.

[54] Geethanjali, P. Myoelectric control of prosthetic hands: state-of-the-art review. *Medical Devices: Evidence and Research* **2016**, 247–255.

[55] Shanmuganathan, V.; Yesudhas, H. R.; Khan, M. S.; Khari, M.; Gandomi, A. H. R-CNN and wavelet feature extraction for hand gesture recognition with EMG signals. *Neural Computing and Applications* **2020**, *32*, 16723 – 16736.

[56] Rodríguez-Tapia, B.; Soto, I.; Marínez, D. M.; Arballo, N. C. Myoelectric Interfaces and Related Applications: Current State of EMG Signal Processing–A Systematic Review. *IEEE Access* **2020**, *8*, 7792–7805.

[57] Sreenivasan, N.; Gutierrez, D. F. U.; Bifulco, P.; Cesarelli, M.; Gunawardana, U.; Gargiulo, G. D. Towards Ultra Low-Cost Myoactivated Prostheses. *BioMed Research International* **2018**, *2018*.

[58] Lindeblad, E.; Nilsson, S.; Gustafson, S.; Svensson, I. Assistive technology as reading interventions for children with reading impairments with a one-year follow-up. *Disability and rehabilitation: assistive technology* **2017**, *12*, 713–724.

[59] Smit, G.; Plettenburg, D. H.; van der Helm, F. C. The lightweight Delft Cylinder Hand: first multi-articulating hand that meets the basic user requirements. *IEEE Transactions on Neural Systems and Rehabilitation Engineering* **2014**, *23*, 431–440.

[60] Heckathorne, C. W. Components for adult externally powered systems. *Atlas of Limb Prosthetics* **1992**,

[61] Chowdhury, R. H.; Reaz, M. B.; Ali, M. A. B. M.; Bakar, A. A.; Chellappan, K.; Chang, T. G. Surface electromyography signal processing and classification techniques. *Sensors* **2013**, *13*, 12431–12466.

[62] OsNoei, M. A.; Hu, H. Myoelectric control systems—A survey. *Biomedical Signal Processing & Control* **2007**, *2*, 275–294.

[63] Chandler, R.; Clauser, C. E.; McConville, J. T.; Reynolds, H.; Young, J. W. *Investigation of inertial properties of the human body*; 1975.

[64] Wang, Y.; Tian, Y.; She, H.; Jiang, Y.; Yokoi, H.; Liu, Y. Design of an Effective Prosthetic Hand System for Adaptive Grasping with the Control of Myoelectric Pattern Recognition Approach. *Micromachines* **2022**, *13*.

[65] World Bank Group, GDP per capita (current USD$). 2021; `https://data.worldbank.org/indicator/NY.GDP.PCAP.CD`.

[66] World Data, The 30 largest and most populous countries. 2022; `https://www.worlddata.info/the-largest-countries.php`.

[67] World Bank Group, GDP per capita (current USD$) - Ecuador | Data. 2021; `https://data.worldbank.org/indicator/NY.GDP.PCAP.CD?locations=EC`.

[68] Dunai, L.; Novak, M.; García Espert, C. Human hand anatomy-based prosthetic hand. *Sensors* **2020**, *21*, 137.

[69] Maat, B.; Smit, G.; Plettenburg, D.; Breedveld, P. Passive prosthetic hands and tools: A literature review. *Prosthetics and orthotics international* **2018**, *42*, 66–74.

[70] Fang, C.; He, B.; Wang, Y.; Cao, J.; Gao, S. EMG-centered multisensory based technologies for pattern recognition in rehabilitation: state of the art and challenges. *Biosensors* **2020**, *10*, 85.

[71] Atasoy, A.; Kaya, E.; Toptas, E.; Kuchimov, S.; Kaplanoglu, E.; Ozkan, M. 24 DOF EMG controlled hybrid actuated prosthetic hand. 2016.

[72] Shi, C.; Yang, D.; Zhao, J.; Jiang, L. i-MYO: A Hybrid Prosthetic Hand Control System based on Eye-tracking, Augmented Reality and Myoelectric signal. *arXiv preprint arXiv:2205.08948* **2022**,

[73] Johansen, D.; Cipriani, C.; Popović, D. B.; Struijk, L. N. Control of a robotic hand using a tongue control system—A prosthesis application. *IEEE transactions on biomedical engineering* **2016**, *63*, 1368–1376.

[74] Vujaklija, I.; Farina, D.; Aszmann, O. C. New developments in prosthetic arm systems. *Orthopedic research and reviews* **2016**, 31–39.

[75] Vincent Systems GmbH, Vincent Hand Evolution 4. 2020; `https://www.vincentsystems.de/vincent-evolution4`.

[76] Feix, T.; Romero, J.; Ek, C. H.; Schmiedmayer, H.-B.; Kragic, D. A metric for comparing the anthropomorphic motion capability of artificial hands. *IEEE transactions on robotics* **2012**, *29*, 82–93.

[77] Williams, W. Ottobock Michelangelo Hand Transcarpal. 2021.

[78] Miguelez, J. M. Clinical experiences with the michelangelo hand, a four-year review. **2011**,

[79] Dunai, L.; Novak, M.; García Espert, C. Human Hand Anatomy-Based Prosthetic Hand. *Sensors* **2021**, *21*.

[80] Medynski, C.; Rattray, B. Bebionic Prosthetic Design. *Myoelectric Symposium* **2011**,

[81] Williams, W. Ottobock Bebionic Hand. 2021.

[82] Connolly, C. Prosthetic hands from touch bionics. *Industrial Robot: An International Journal* **2008**,

[83] Össur Company, i-Limb® Quantum Bionic Hand. 2020.

[84] others,, *et al.* A low cost anthropomorphic prosthetic hand using DC micro metal gear motor. **2016**, 42–46.

[85] Melo, J. L. In *Ergonomía Practica*; Mapfre, F., Ed.; 2009; Vol. 1; pp 1–192.

[86] Quinn, E. Generally Accepted Values for Normal Range of Motion (ROM) in Joints. 2023; `https://www.verywellhealth.com/what-is-normal-range-of-motion-in-a-joint-3120361`.

[87] Juarez, D.; Peydro, M. A.; Mengual, A.; Ferrándiz, S. A review of concurrent engineering. *Annals of the Oradea University: Fascicle Management and Technological Engineering* **2015**, 94–97.

[88] Rihar, L.; Žuek, T.; Kuar, J. How to successfully introduce concurrent engineering into new product development? *Concurrent Engineering* **2020**, *29*, 87 – 101.

[89] Kumar, R.; Roopa, A.; Sathiya, D. P. Arduino ATMEGA-328 microcontroller. *Int. J. Innov. Res. Electr. Electron. Instrum. Control Eng* **2015**, *3*, 27–29.

[90] Shen Meng, X. S. Design and Implementation of Long-Term Single-Lead ECG Monitor. *Journal of Biosciences and Medicines* **2015**, *3*, 18.

[91] Mendes Junior, J. J. A.; Campos, D. P.; Biassio, L. C. d. A. V. D.; Passos, P. C.; Júnior, P. B.; Lazzaretti, A. E.; Krueger, E. AD8232 to Biopotentials Sensors: Open Source Project and Benchmark. *Electronics* **2023**, *12*, 833.

[92] Vieira, T. M.; Botter, A. The accurate assessment of muscle excitation requires the detection of multiple surface electromyograms. *Exercise and Sport Sciences Reviews* **2021**, *49*, 23–34.

[93] Setty, K.; van Niekerk, T.; Stopforth, R. Design Considerations of the Touch Hand 4. *Procedia CIRP* **2020**, *91*, 494–502.

[94] Setty, K.; Van Niekerk, T.; Stopforth, R.; Sewsunker, K.; du Plessis, A. Design and kinematic analysis of a multi-grip hand—touch hand 4. *Int J Mech Eng Robot Res* **2022**, *11*, 466–78.

[95] Markforged, C. Comparison between PLA, ABS and nylon. 2021; `https://markforged.com/es/resources/blog/pla-abs-nylon`.

[96] Chonga, S.; Chiub, H.-L.; Liaob, Y.-C.; Hungc, S.-T.; Pand, G.-T. Cradle to Cradle® design for 3D printing. *Chemical Engineering* **2015**, *45*.

[97] Alkhatib, F.; Cabibihan, J.-J.; Mahdi, E. Data for benchmarking low-cost, 3D printed prosthetic hands. *Data in Brief* **2019**, *25*, 104163.

[98] Alkhatib, F.; Cabibihan, J.-J.; Mahdi, E. Data for benchmarking low-cost, 3D printed prosthetic hands. *Data in brief* **2019**, *25*, 104163.

[99] Mata Amritanandamayi Devi,; Udupa, G.; Sreedharan, P. A novel underactuated multi-fingered soft robotic hand for prosthetic application. *Robotics and Autonomous Systems* **2018**, *100*, 267–277.

[100] de Almeida Regina, B.; Aguiar, M. J. R.; Ferreira, A. A. Comprehensive and Didactic DC Servo-motor Control Platform. **2019**, 1–6.

[101] Fajardo, J.; Ferman, V.; Cardona, D.; Maldonado, G.; Lemus, A.; Rohmer, E. Galileo hand: An anthropomorphic and affordable upper-limb prosthesis. *IEEE access* **2020**, *8*, 81365–81377.

[102] Bolanakis, D. E. A Survey of Research in Microcontroller Education. *Revista Iberoamericana de Tecnologias del Aprendizaje* **2019**, *14*, 50–57.

[103] Awad, S. F.; Kadhim, F.; Aboud, W.; Tahi, M. A.-D. Strain and deformation measurement for prosthetic parts using the Arduino microcontroller and strain gauges instruments. *Int. J. Mech. Eng* **2022**, *7*, 1049–1055.

[104] Chinbat, O.; Lin, J.-S. Prosthetic arm control by human brain. **2018**, 54–57.

[105] Wallace, S.; Richardson, M.; Donat, W. *Getting started with raspberry pi*; Maker Media, Inc., 2021.

[106] Ehrmann, G.; Blachowicz, T.; Homburg, S. V.; Ehrmann, A. Measuring Biosignals with Single Circuit Boards. *Bioengineering* **2022**, *9*.

[107] Gstoettner, C.; Salminger, S.; Bergmeister, K.; Willensdorfer, A.; Aman, M.; Aszmann, O. C. In *Bionic Limb Reconstruction*; Aszmann, O. C., Farina, D., Eds.; Springer International Publishing: Cham, 2021; pp 137–146.

[108] Geethanjali, P. Myoelectric control of prosthetic hands: state-of-the-art review. *Medical Devices: Evidence and Research* **2016**, *9*, 247–255.

[109] Rayo, A. G. S.; Gómez, L. H. H.; Sánchez, A. T. V.; Fernández, J. A. B.; Campos, J. A. F.; Calderón, G. U.; Rayo, V. M. S.; Peñaloza, A. E. F. Design and manufacturing of a dry electrode for EMG signals recording with microneedles. *Improved Performance of Materials: Design and Experimental Approaches* **2018**, 259–267.

[110] Devices, A. Single-Lead, Heart Rate Monitor Front End - AD8232 Data Sheet. 2020; `www.analog.com`.

[111] Luchetti, M.; Cutti, A. G.; Verni, G.; Sacchetti, R.; Rossi, N. Impact of Michelangelo prosthetic hand: Findings from a crossover longitudinal study. *Journal of Rehabilitation Research & Development* **2015**, *52*.

[112] Egbuhuzor, M.; Nwafor, S.; Umunnakwe, C.; Egoigwe, S. *Thin Films-Deposition Methods and Applications*; IntechOpen, 2023.

[113] Pierozynski, B. On the low temperature performance of nickel-metal hydride (NiMH) batteries. *Int. J. Electrochem. Sci* **2011**, *6*, 860–866.

[114] Olabi, A. G.; Abbas, Q.; Shinde, P. A.; Abdelkareem, M. A. Rechargeable batteries: Technological advancement, challenges, current and emerging applications. *Energy* **2023**, *266*, 126408.

[115] Cabibihan, J.-J.; Abu Basha, M. K.; Sadasivuni, K. Recovery behavior of artificial skin materials after object contact. **2016**, 449–457.

[116] Mushtaq, R. T.; Iqbal, A.; Wang, Y.; Rehman, M.; Petra, M. I. Investigation and Optimization of Effects of 3D Printer Process Parameters on Performance Parameters. *Materials* **2023**, *16*.

[117] Tran, P. *SOLIDWORKS 2022 Advanced Techniques: Mastering Parts, Surfaces, Sheet Metal, SimulationXpress, Top-Down Assemblies, Core & Cavity Molds*; SDC publications, 2021.

[118] Munford, P.; Normand, P. *Mastering Autodesk Inventor 2016 and Autodesk Inventor LT 2016: Autodesk Official Press*; John Wiley & Sons, 2015.

[119] Verma, G. *Autodesk fusion 360 black book*; BPB Publications, 2018.

[120] Saeed, B.; Zia-ur Rehman, M.; Gilani, S. O.; Amin, F.; Waris, A.; Jamil, M.; Shafique, M. Leveraging ANN and LDA classifiers for characterizing different hand movements using emg signals. *Arabian Journal for Science and Engineering* **2021**, *46*, 1761–1769.

[121] Bergil, E.; Oral, C.; Ergul, E. U. Efficient hand movement detection using k-means clustering and k-nearest neighbor algorithms. *Journal of Medical and Biological Engineering* **2021**, *41*, 11–24.

Chapter 7

Annexes

CAD model and Kinematic scheme for thumb, index, middle, ring and little fingers
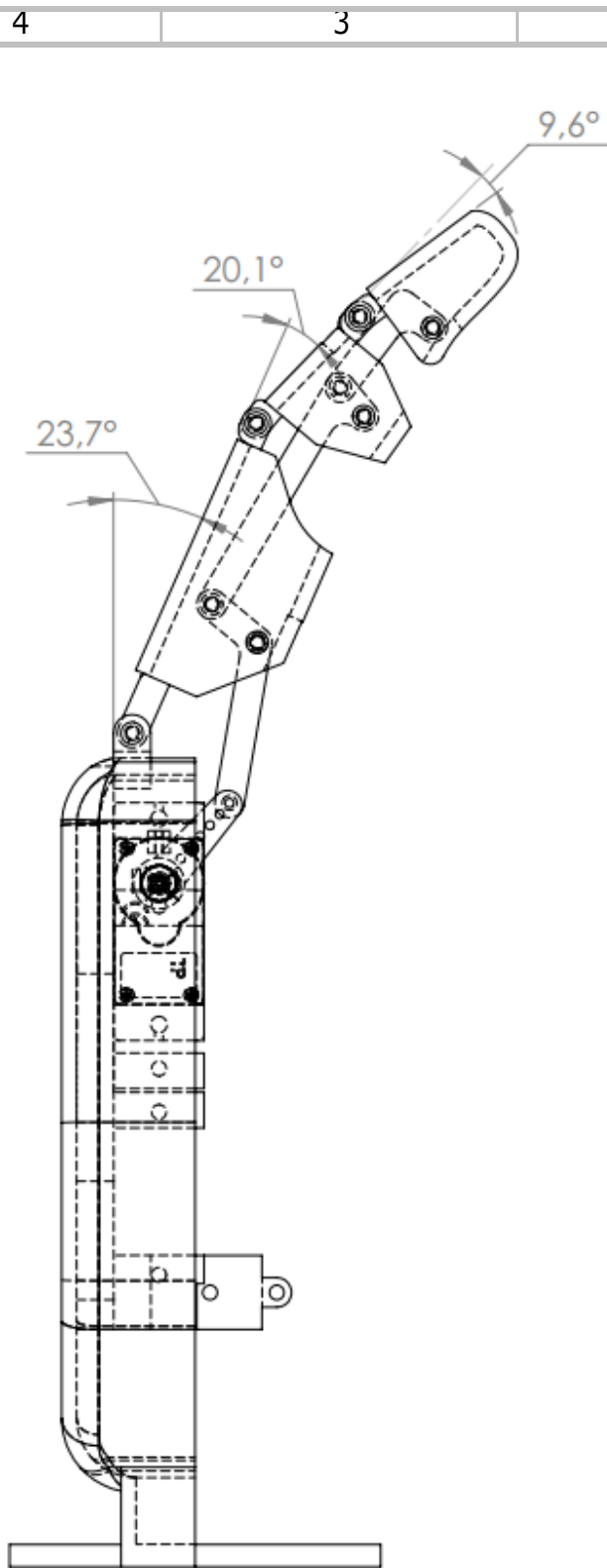
4   3   2   1

F   F
E   E
D   D
C   C
B   B
A   A

49,4°

8,8°
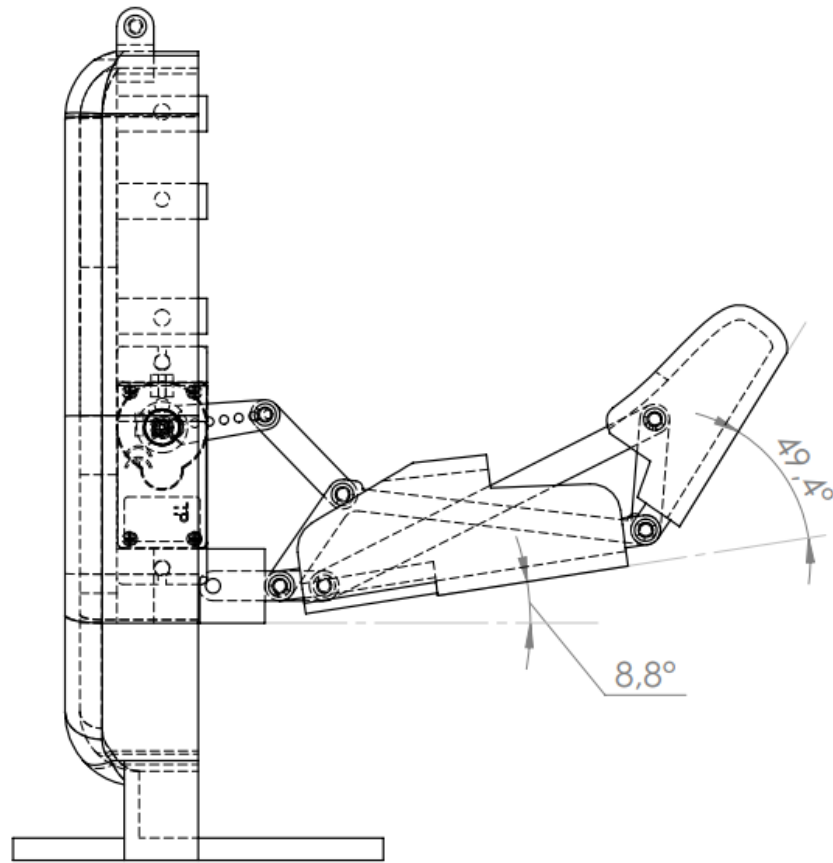
Thumb finger angles
Scale 1:1
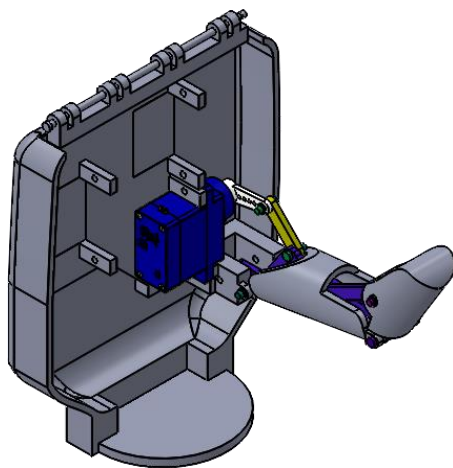
Isometric view
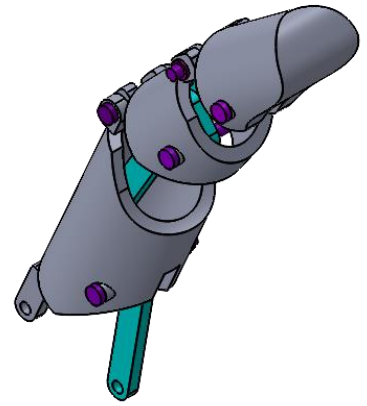Palm - Thumb finger
Scale 1:2
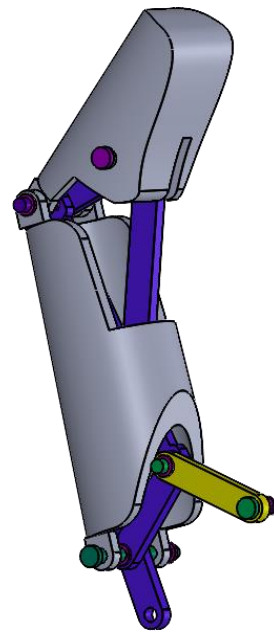
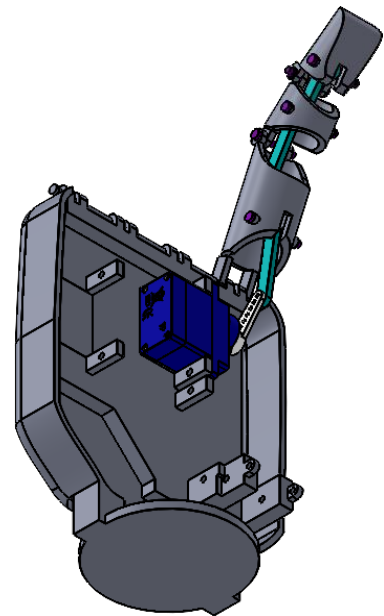Isometric view
Thumb finger
Scale 1:1

Thumb Finger Angles
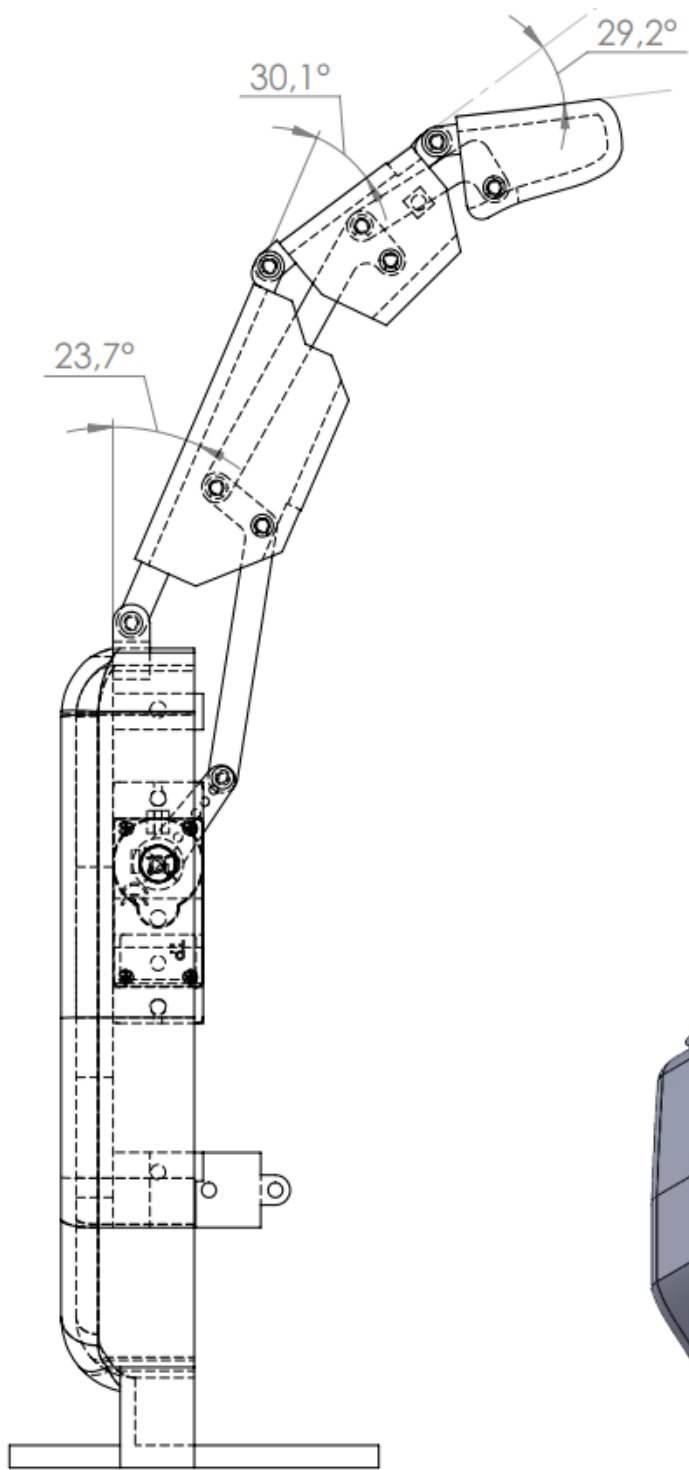
9,6°

20,1°

23,7°

Index finger angles
Scale 1:1

Isometric view
Index finger
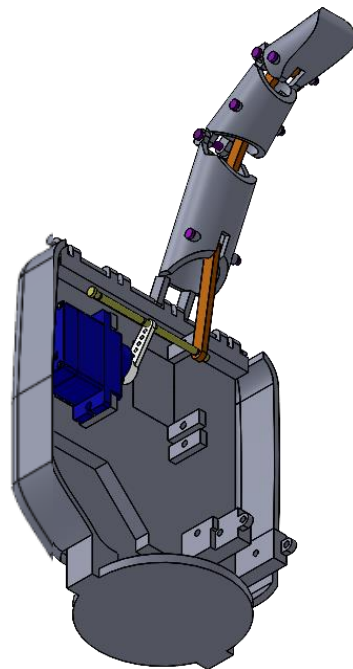Scale 1:1

Isometric view
Palm - Index finger
Scale 1:2

Index Finger Angles

29,2°

30,1°
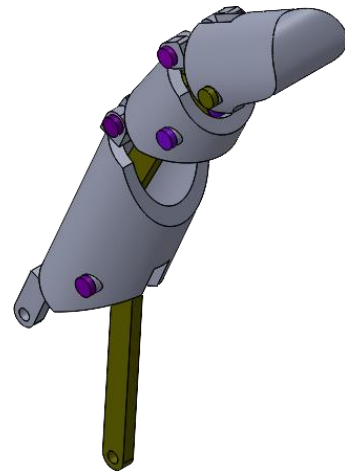
23,7°

Middle finger angles
Scale 1:1

Isometric view
Middle finger
Scale 1:1
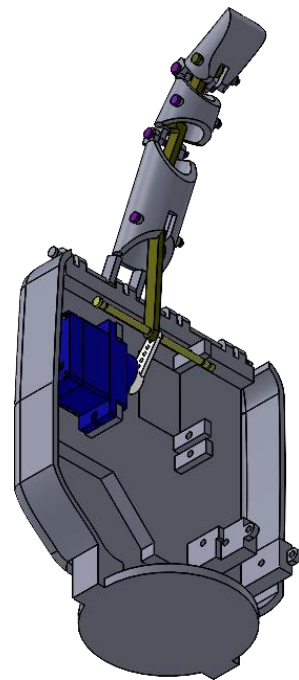
Isometric view
Palm - Middle finger
Scale 1:2

Middle Finger Angles
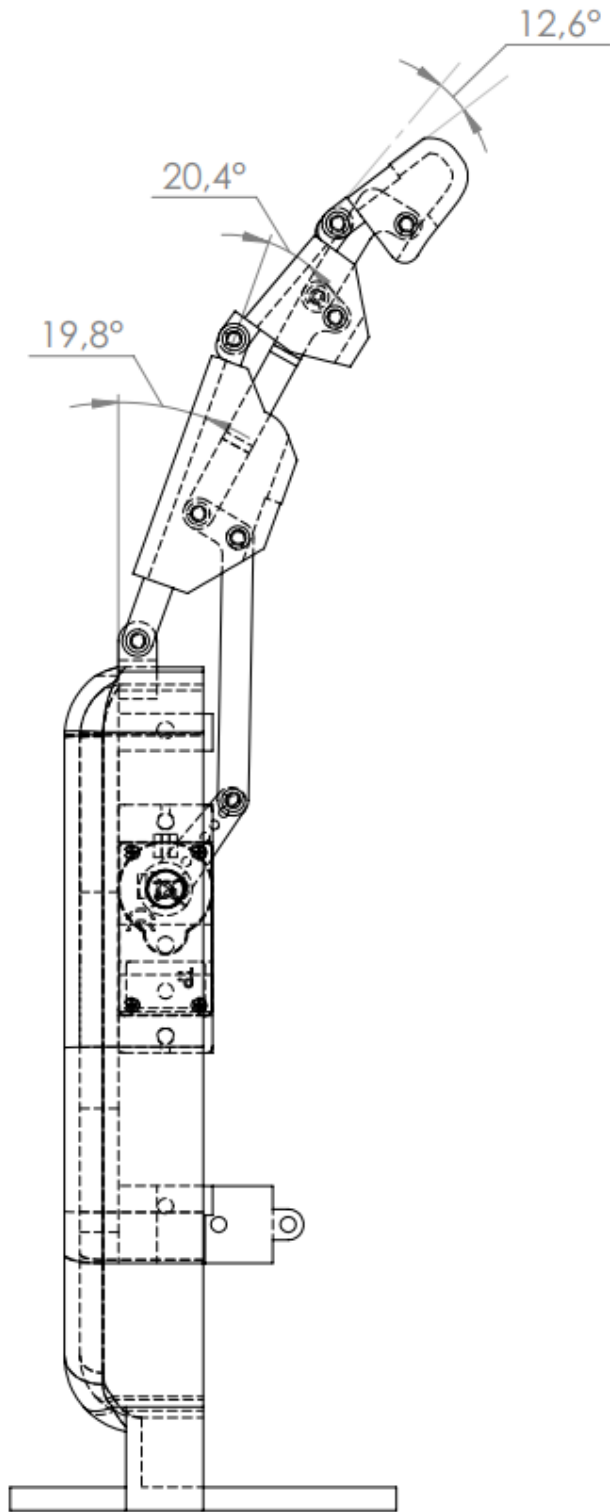
26,4°

11,1°

23,5°
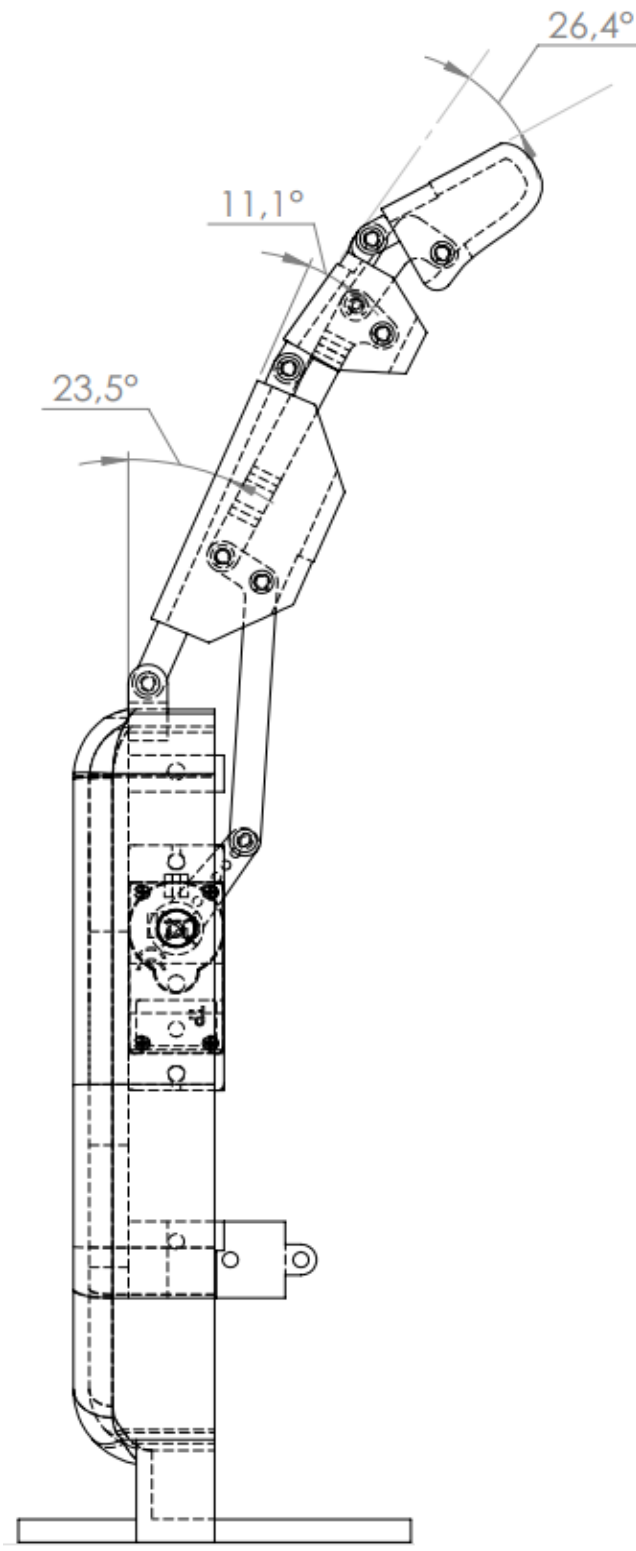
Ring finger angles
Scale 1:1

Isometric view
Ring finger
Scale 1:1

Isometric view
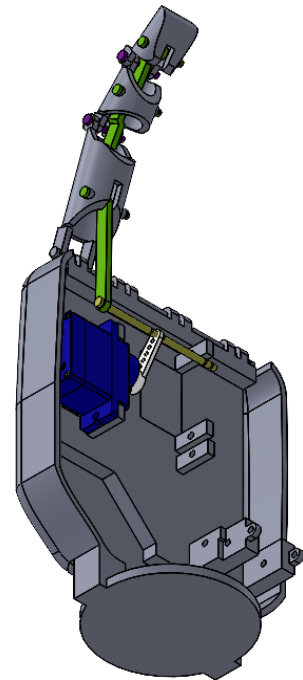Palm - Ring finger
Scale 1:2

Ring Finger Angles

12,6°

20,4°

19,8°

Little finger angles
Scale 1:1

Isometric view
Little finger
Scale 1:1

Isometric view
Palm - Little finger
Scale 1:2

Little Finger Angles

| 4 | 3 | 2 | 1 |

F
E
D
C
B
A